The EU FP7 NanoDefine Project

Development of an integrated approach based on validated and standardized methods to support the implementation of the EC recommendation for a definition of nanomaterial

Protocols for preparation of products for microscopy methods

NanoDefine Technical Report D2.4

Toni Uusimäki and Philippe Hallegot

The NanoDefine Consortium 2016

The research leading to these results has received funding from the European Community's Seventh Framework Programme (FP7/2007-2013) under Grant Agreement n° 604347

NanoDefine in a nutshell:

The EU FP7 NanoDefine project was launched in November 2013 and will run until October 2017. The project is dedicated to support the implementation of the EU Recommendation on the Definition of Nanomaterial by the provision of the required analytical tools and respective guidance. Main goal is to develop a novel tiered approach consisting of (i) rapid and cost-efficient screening methods and (ii) confirmatory measurement methods. The "NanoDefiner" eTool will guide potential end-users, such as concerned industries and regulatory bodies as well as enforcement and contract laboratories, to reliably classify if a material is nano, or not. To achieve this objective, a comprehensive inter-laboratory evaluation of the performance of current characterisation techniques, instruments and software is performed. Instruments, software and methods are further developed. Their capacity to reliably measure the size of particulates in the size range 1-100 nm and above (according to the EU definition) is validated. Technical reports on project results are published to reach out to relevant stakeholders, such as policy makers, regulators, industries and the wider scientific community, to present and discuss our goals and results, to ensure a continuous exchange of views, needs and experiences obtained from different fields of expertise and application, and to finally integrate the resulting feedback into our ongoing work on the size-related classification of nanomaterials.

Bibliographic data:

NanoDefine Technical Report D2.4

Protocols for preparation of products for microscopy methods

Author(s): Uusimäki, T.* [a], Hallegot, P.[b]

Contributor(s): Kägi, R.[a] , Loeschner, K.[c]

Affiliation(s): [a] Eawag, Überlandstrasse 133, 8600, Dübendorf, Switzerland

[b] Laboratoire de Microscopie Electronique, L'Oréal, 1 avenue Eugène Schueller, BP 22, 93601 Aulnay Sous Bois Cedex France

[c] Technical University of Denmark, National Food Institute, Building B, Moerkhoej Bygade 19, DK-2860 Soeborg, Denmark

Publication date: 04/02/2016

Publisher: The NanoDefine Consortium

Place of publication: Wageningen, The Netherlands

Citation: Uusimäki, T., Hallegot, P., Protocols for preparation of products for microscopy methods, NanoDefine Technical Report D2.4, NanoDefine Consortium, Wageningen, 2016

URL: http://www.nanodefine.eu/index.php/downloads/public-deliverables

Contact: coordinator@nanodefine.eu, www.nanodefine.eu

* Corresponding author: ToniMikael.Uusimaeki@eawag.ch

Table of Contents

Index of Figures

1 Abbreviations and Acronyms

BF	Bright Field
DF	Dark Field
EC	European Commission
EDS	Energy Dispersive X-ray Spectroscopy
EM	Electron Microscopy
ESEM	Environmental SEM
ET	Electron Tomography
FIB	Focused Ion Beam
HAADF	High Angle Annular Dark Field
IBID	Ion Beam Induced Chemical Vapour Deposition
NP	Nanoparticle(s)
PE	Polyethylene
PSD	Particle Size Distribution
RT	Room Temperature
SE	Secondary Electron
SEM	Scanning Electron Microscopy
SIRT	Simultaneous Iterative Reconstruction Technique
SLS	Static Light Scattering
SOP	Standard Operating Procedure
STEM	Scanning Transmission Electron Microscopy
TEM	Transmission Electron Microscopy
TSEM	Scanning Electron Microscopy in Transmission Mode
UM	Ultramicrotomy
WP	Work Package

2 Summary

This report describes the methods and protocols available for sample preparation of nanoparticle (NP) containing products within the field of electron microscopy (EM). Since sample preparation of products are considered in D2.6 (separation of the matrix and particles) and deposition methods for EM carriers in D2.5, the focus here is on solid samples that are not dispersible in carrier liquids (e.g. coatings, plastics and concrete). The protocols and methods described here were developed using the hematite (Fe_2O_3) NPs embedded within a high density polyethylene (PE) carrier matrix, provided by the NanoDefine (ND) consortium as an example for a solid sample. In addition, the challenges of the extraction of NPs from cosmetics for EM characterization are explored using different sample preparation methods. Special attention is given to scanning electron microscopy (SEM) and transmission electron microscopy (TEM), which are relevant Tier 2 metrologies for the EC definition of a nanomaterial.

3 Introduction

Several highly sophisticated EM sample preparation techniques have been developed over the last decades to account for a large variety of sample properties. In this report, we discuss and evaluate methods that are commonly available to most EM centers. Scanning electron microscopy (SEM) uses a finely focused electron beam scanning over the surface of the investigated material in a high vacuum chamber. The materials have to be suitable for high vacuum environment (pressures typically in the order of 10^{-5} – 10^{-7} mbar) and should be coated with an electrically conductive layer (e.g. C or Au) to avoid charging effects caused by the incoming electrons. However, newer microscopes operated at low acceleration voltages (1-2 kV or below) or variable pressure microscopes do not require conductive samples anymore. In addition, sensitivity to the electron beam and sample contamination during the analysis often limit the performance of EM. For transmission electron microscopy (TEM) the samples have to be transparent for the electron beam and thus need to be extremely thin (5 -300 nm).

The magnetic properties of nanocomposites can be tuned for a variety of applications ranging from biomedicine to electronics by embedding magnetic NPs such as hematite into a PE matrix (Ruiz, 2009). On the other hand, hematite nanoparticles are frequently used in the polymer industry as pigments (pigment red 101) to change the base colour of the PE. The material chosen for ND was manufactured by industrial partners and, as received as small cylinder shaped rods (Figure 1). The dimensions of the rods were ~ 2 mm x 5 mm. The mass ratio of the hematite nanoparticles was 5% (g/g). The NPs were ~ 40 nm in diameter and were agglomerated into complex 3D structures. In addition to the Fe_2O_3 in PE, pure PE material without the NPs and a powder containing exclusively the Fe_2O_3 NPs were distributed. These samples were used for the pre-characterization of the materials.

Figure 1 Fe_2O_3/PE rods on a 3 cm diameter filter paper.

Mineral particles are used in cosmetics, for example for UV filtering or colouring purpose. Some UV-filtering particles have nano-dimensions and the corresponding raw materials can be classified as nanomaterial or non-nanomaterial, depending on the proportion of nanoparticles present in the material. The European Union introduced directives in relation to nanomaterials in cosmetics regulation (1223/2009), among them the labelling of nanomaterials incorporated in the product. This labelling is supported by the analyses of the raw materials used during formulation. However, in what extent could we determine, from the analysis of a finished product, for control purpose for example, if a nanomaterial has been incorporated?

4 Fe_2O_3 Nanoparticles in Polyethylene Matrix (solid matrix)

This chapter focuses on sample preparation methods for the iron oxide nanoparticles embedded in polyethylene matrix for EM characterization needs.

4.1 Pre-Characterizations

The pure iron oxide powder was mixed with MilliQ water and sonicated (BAM). A 3 µl drop was placed on top of a TEM grid and after 5 minutes of incubation, the excess liquid was removed. Figure 2 shows the SEM image of the NPs recorded in transmission mode (TSEM). A PSD (Feret min) was derived from the manual measurement of individual particles (median = 34.55 nm, N = 170 particles). The NPs are agglomerated into complex 3D structures making the identification of the primary constituents extremely challenging.

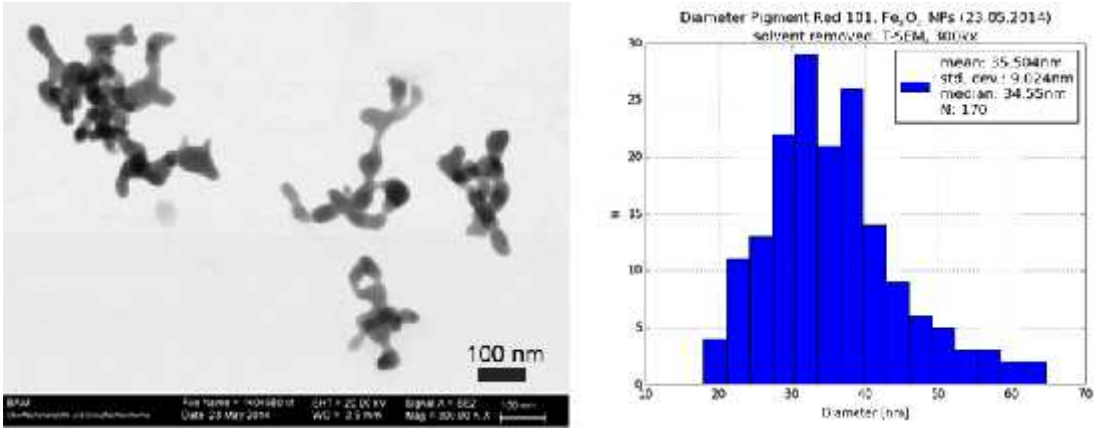

Figure 2 TSEM image of iron oxide NP agglomerates (left) and the PSD derived from the measurements of individual primary particles (right).

PE pellets without the iron oxide NPs were fixed with a silver paste to a SEM holder (Figure 3(a)) and coated with a thin layer of carbon (BAM). On the surface of the PE pellets no iron oxide particles were found. Also after heating the sample in muffle furnace (500°C, 1h) no residue particles were found.

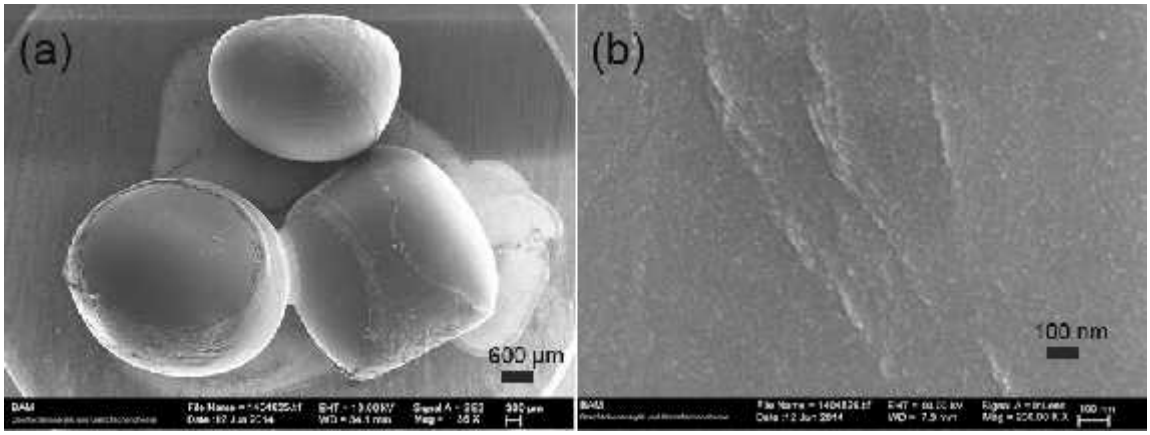

Figure 3 (a) SEM image of the PE pellets. (b) The surface recorded at higher magnification. No iron oxide particles were observed at the surface of the PE pellets.

To confirm the presence of iron oxide in the Fe_2O_3/PE rods a thin slide of the sample was prepared by ultramicrotomy (UM, chapter 4.3). Individual Fe_2O_3 particles were identified based on energy dispersive X-ray spectroscopy in STEM mode (STEM-EDS, EAWAG) with the electron probe scanning only on the hematite NP agglomerate shown in figure 4, which was recorded using high angle annular dark field (HAADF) mode. A Hitachi HD2700 operating at 200 kV was used for all STEM images unless otherwise stated. The X-ray spectrum shows clear presence of iron and oxygen. A quantitative analysis to differentiate between magnetite (Fe_3O_4) and hematite is very challenging due to interferences of the electron beam with the oxygen containing PE matrix. The copper peak results from the TEM grid, which was made of Cu. The silicon (Si) signal is present throughout the TEM grid and possibly represents a contamination resulting from either the manufacturing process of the TEM grids or from their storage.

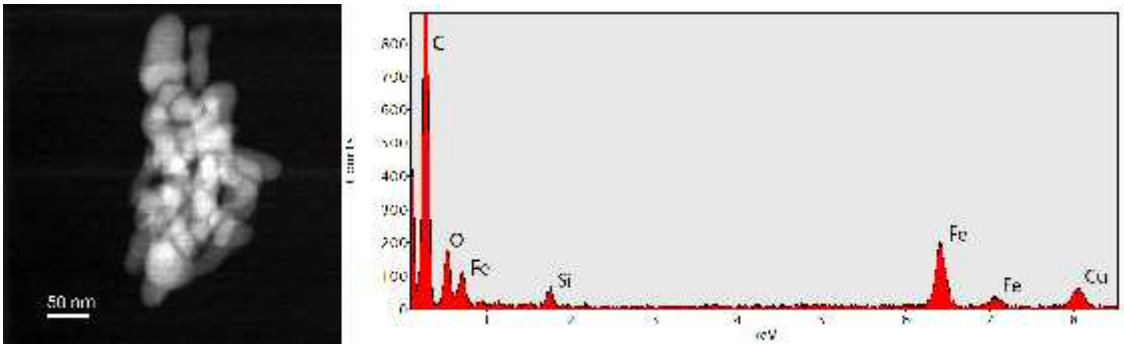

Figure 4 HAADF-STEM image of an iron oxide NP agglomerate and the corresponding X-ray spectrum.

A simple and straightforward extraction of the hematite NPs from the Fe_2O_3/PE rods is by thermal degradation. A muffle furnace was used to burn the PE away (BAM, 500°C, 1h). Residue of the PE was found not to be present and the remaining was a red powder, which was mixed with MilliQ water and sonicated. A drop of 3 µl of the solution was drop casted onto TEM grid and waited until dry. TSEM image of one of the particles is given in figure 5 alongside with the PSD analysis. 76 particles were manually analysed (Feret min) and a median of 33.15 nm was measured. However, thermal decomposition is not applicable to all filler materials, and the effect to the size and structure of the Fe_2O_3 NPs is unknown. It has been reported, that hematite has a phase transition to magnetite under thermal treatment (375°C) in the presence of H_2 (as in PE) (Gaviría, 2007). Hence, sample preparation methods to image the Fe_2O_3 NPs directly within the PE was further tested.

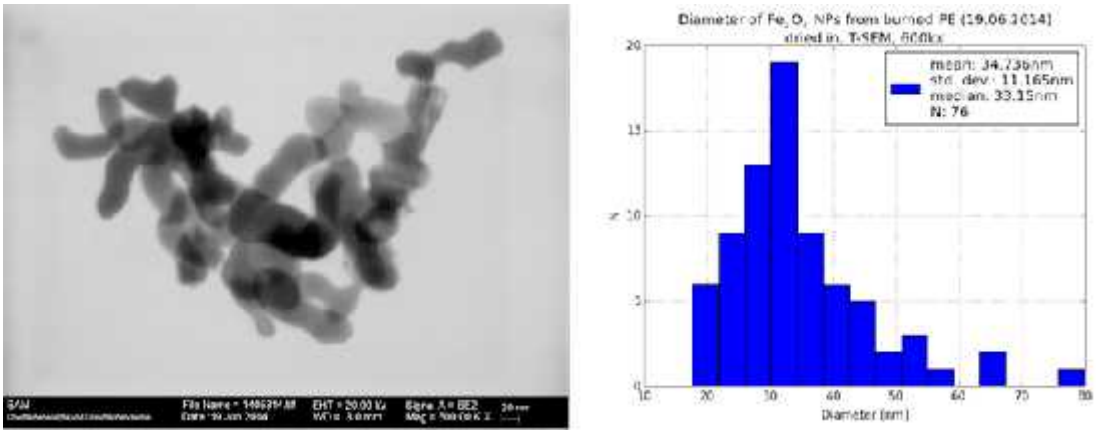

Figure 5 TSEM image of an iron oxide NP agglomerate and the PSD.

4.2 Focused Ion Beam

The focused ion beam (FIB) technique allows the fabrication of thin lamellas (5 – 300 nm) from bulk materials. Dual-Beam FIB/SEM provides simultaneous imaging with the electron beam while manipulating the sample (milling/deposition) using the ion beam (Young, 2005). TEM lamellas can be crafted from selected sample sites and later transferred to TEM grids. Here a FEI Helios 600i was used to prepare a thin lamella from the Fe_2O_3/PE composite material for NP size analysis. As seen in Figure 6, first a protective platinum (Pt) layer was deposited onto the selected sample area and then a trench was milled adjacent to the Pt layer. The TEM lamella was glued to a sharp needle (omniprobe) using ion beam induced chemical vapour deposition (IBID). The TEM lamella was then cut and transferred to TEM grid (Figure 7(a)). Final polishing of the lamella was done using low ion currents (8 pA) until a thickness of ~ 150 nm was reached.

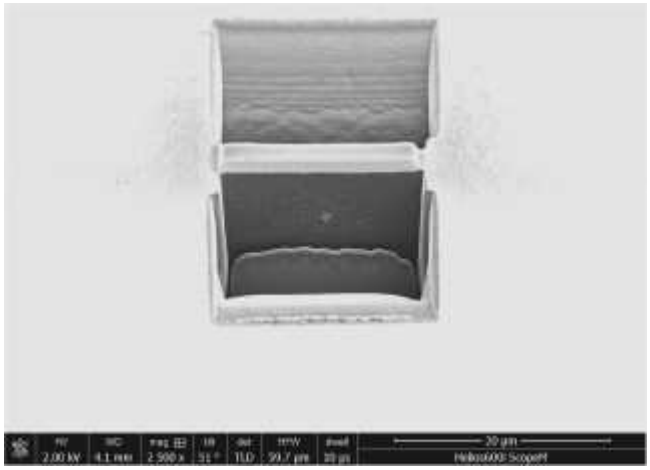

Figure 6 SE image of the milled lamella with platinum protection layer shown on top.

Although FIB is a highly versatile instrument for most TEM characterization demands, PE introduced difficulties related to bending and melting of the PE matrix due to the ion beam induced heating (Figure 7(a), white arrow). Due to these constrains, large and thin enough lamellas are difficult to fabricate

using the FIB. However, such lamellas are needed to derive a statistically reliable particle size distribution (PSD) of the Fe_2O_3 NPs in the PE matrix. In our samples, only a few Fe_2O_3 NP agglomerates were observed (Figure 7(b)), which did not allow to establish a reliable PSD.

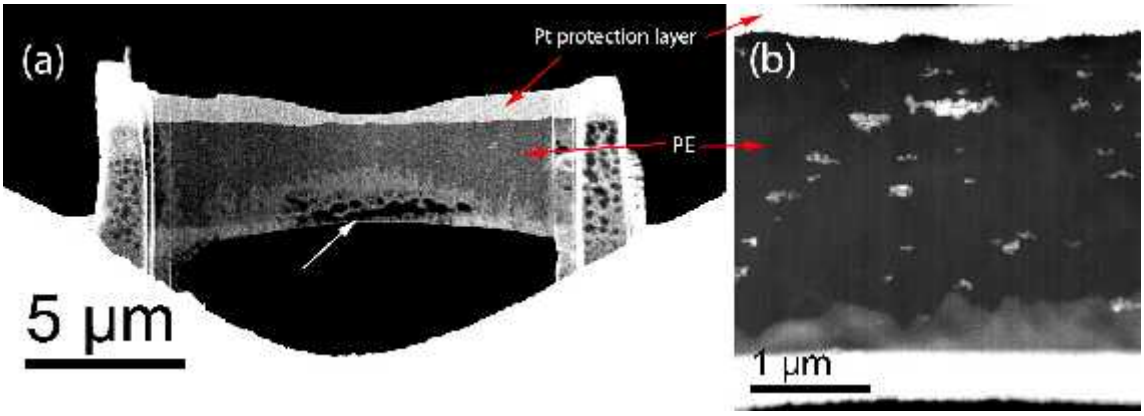

Figure 7 (a) HAADF-STEM image of a lamella attached to TEM grid. (b) HAADF-STEM image recorded at higher magnification revealing Fe_2O_3 NP agglomerates dispersed in the PE matrix.

To reduce bending and melting effects a thicker (~ 500 nm) and larger (100 x 25 µm) lamella was fabricated (Figure 8, left). The PE was still electron transparent, but due to the depth of field of the electron beam, it was not possible to properly image all agglomerates in the sample in one image (Figure 8, right). The distinction between particles in focus and particles out of focus, is extremely challenging using automated image analysis routine. Due to this and for probable overlapping of the agglomerates, thick lamellas are not suitable to establish PSD of NPs dispersed in solid matrices.

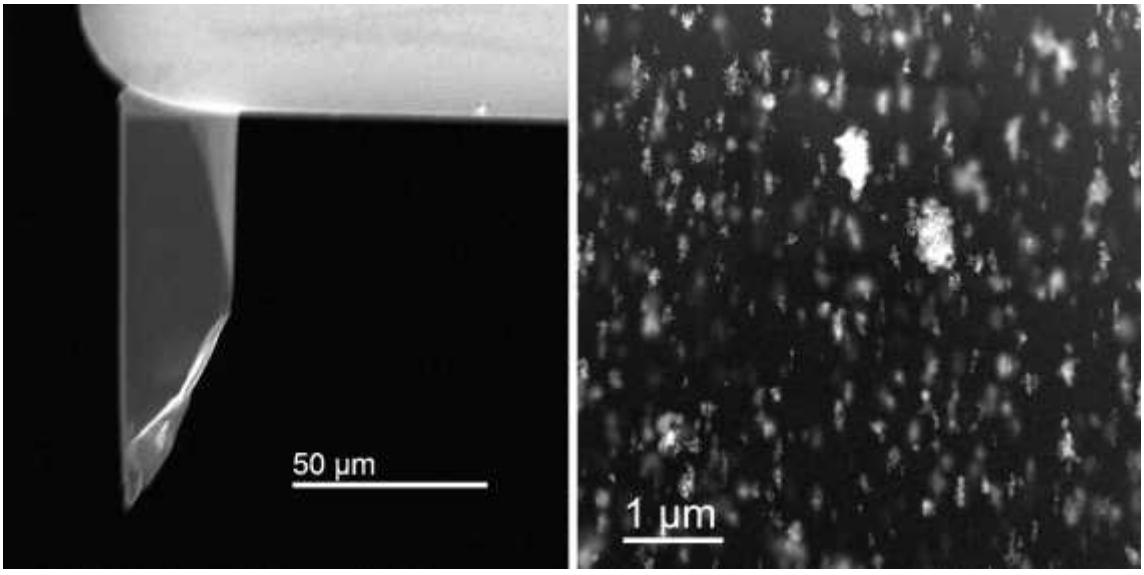

Figure 8 Left: SE-STEM image of a thick knife shaped lamella attached to a TEM grid. Right: HAADF-STEM image recorded at higher magnification of the Fe_2O_3 NP agglomerates.

4.3 Ultramicrotomy

For soft materials such as biological specimens or plastics, ultamicrotomy (UM) provides fast, economical and simple sample preparation method for the fabrication of thin electron transparent sections used in TEM characterization. Usually, the sample is first embedded in epoxy resin and trimmed to obtain a cutting edge. Ultrathin sections (50 – 300 nm) are then cut using a diamond knife. The sample and knife temperature can be adjusted from room temperature to cryo conditions (~ -140 °C). The sections are left floating in water and later retrieved onto TEM grids. Artefacts and deformations to the specimen due to heat or compression are often difficult to distinguish from real structures. (Gnägi, 2008)

4.3.1 Inter-Laboratory Comparison

Within the ND consortium, three laboratories (BASF, CODA-SERVA and EAWAG) investigated the Fe_2O_3/PE sample using UM with different experimental parameters, which are detailed in the appendix A. Representative TEM images (Figure 9) show a feature, which was present in all of the samples. Cutting with a diamond knife strained and compressed the ultra-thin PE slices, which resulted in crushed sections with a wavy structure. It follows, that the difference in height of the iron oxide particles embedded within the oscillating PE section was way beyond the depth of field of the electron beam, resulting in images where some of the Fe_2O_3 NP agglomerates were in focus, but others were out of focus and appeared blurred comparable to (Figure 8, right). The wavy structure of the PE sections was present with thicknesses up to 400 nm and was diminished at 600 nm, which is however too thick for TEM analysis. Additionally the Fe_3O_4/PE rods were sent to an ultramicrotomy specialist company Diatome AG (Biel, CH), who reported similar issues in addition to damage to the cutting knife.

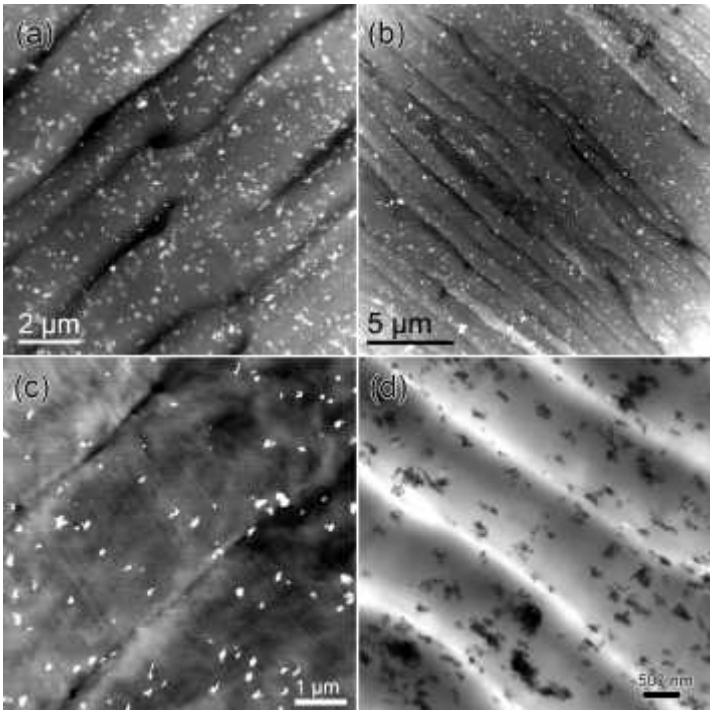

Figure 9 (a) HAADF-STEM image of a UM section (EAWAG, RT). (b) HAADF-STEM image of a UM section (EAWAG, cryo). (c) HAADF-STEM image of a UM section (BASF). (d) BF-TEM image

of a UM section (CODA-SERVA).

The large field of view of the BF-TEM mode enables the analysis of the images as in figure 9(d). However the tools provided by default ImageJ software are not able to separate agglomerates into primary constituents, which was also stated in the internal analysis report (CODA-SERVA). This leads to ferret minimum values of the whole agglomerates and is by far too large, as seen in figure 10, where the segmentation results are also visible.

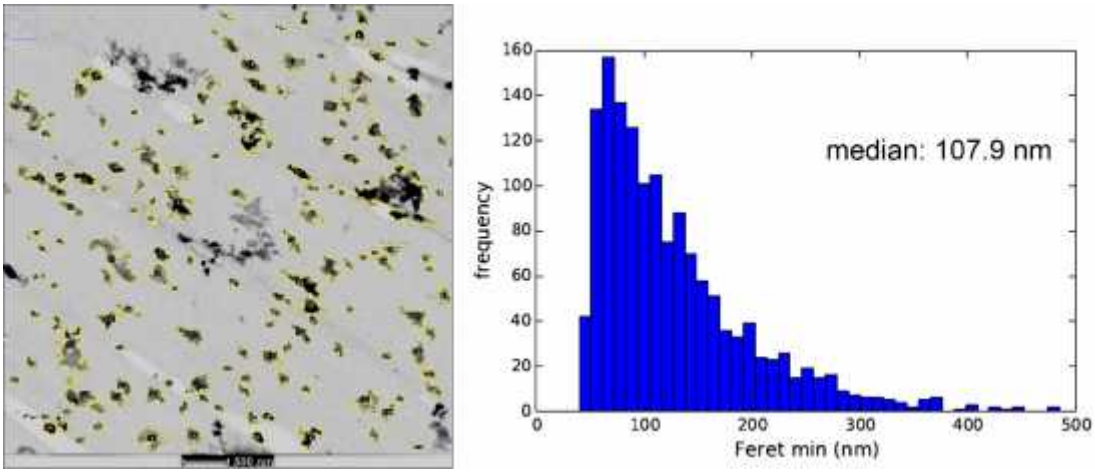

Figure 10 BF-TEM image of a UM section with iron oxide NP agglomerates and the PSD.

4.3.2 Low Temperature Thermal Treatment

The best results were accomplished by heating the UM sections on a TEM grid. A heater (Gerhardt Hotplate) was used having the TEM grids lying on a clean SEM aluminium pin mount specimen holder. The grids were first heated to 80°C temperature for 20 minutes, then the temperature was raised to 112°C for 20 minutes and finally 130°C for 20 minutes. The temperature was measured by direct contact of a K type thermocouple using a Voltcraft IR 900-30S thermometer. The wavy PE structure was minimized and all particles were located at comparable heights. Thus all Fe_3O_4 agglomerates were successfully imaged in focus. The primary particle site can be extracted from such images using standard image analysis routines (Figure 11(a)). Based on 20 HAADF-STEM images, the PSD including 2383 primary constituents was derived (Figure 10(b)).

The NanoDefine ParticleSizer developed within work package 5 was used for the segmentation and analysis in a fully automatic mode.[1] The distribution was fitted using Matlab program with a log-normal curve. The fitted mean value for the Feret minimum was 41.3 nm and the median calculated directly from the data was 37.3 nm, a clear indication of a nanomaterial according to EC definition. Figures 10(c) and 10(d) show details of the segmentation results. The automatic segmentation pipeline very accurately identified primary particles, although a few mismatches were obtained due to the complex 3D structure of the agglomerated particles (Figure 11(c) and 11(d), white arrows). Pragmatically, such difficult structures can be manually omitted in the NanoDefiner tool. To investigate the real 3D structure of the agglomerated particles, electron tomography (ET) analysis of individual agglomerates was performed and the results are discussed in chapter 8.

1) All else default values, except min OTB difference = 5, use irregular watershed structures = TRUE, single particle mode = FALSE, IWS convexity threshold = 0.88, minimal feret min = 6.

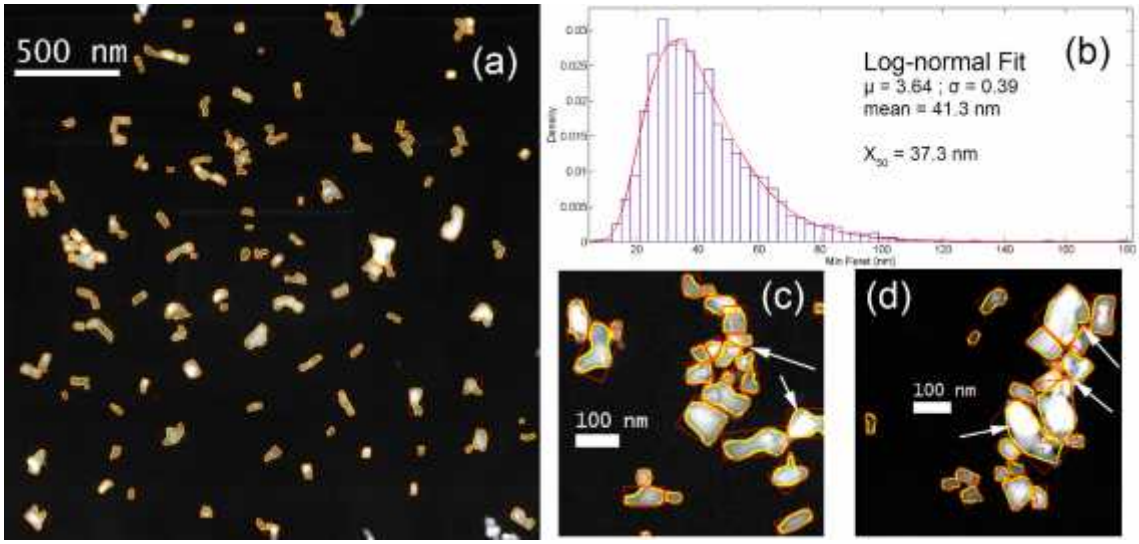

Figure 11 (a) HAADF-STEM image of the hematite NPs with segmentation results. (b) PSD with mean and median values. N = 2383. (c) and (d) zoomed in images showing false segmentation outputs indicated by white arrows.

4.4 Electron Tomography

Electron tomography (ET) is a method similar to MRI or CT imaging, to reveal the 3D representation of the object through a series of projection images. MRI and CT can access objects on the millimetre to micrometre scale and are thus not suitable for the analysis of nanoscale structures. However using ET one can reach to atomic resolutions. In ET the sample is tilted using the goniometer of the TEM, and images are recorded at increasing tilt angles to acquire a so-called tilt series. After the alignment of the tilt series, the object can be reconstructed using mathematical algorithms (inverse radon transform). Although various reconstruction methods exist, usually the weighted back projection or simultaneous iterative reconstruction technique (SIRT) are used. For a quantitative analysis, the 3D reconstruction has to be segmented to separate the objects of interest from the background of the 3D image. In material science, pillar-shaped samples are usually prepared from bulk specimens to maximize the tilt range and to achieve a constant thickness at all tilt angles. (Midgley, 2009)

4.4.1 Sample Preparation and Analysis

To compare the 2D measured size of the Fe_2O_3 NPs embedded in the PE matrix obtained from the UM sections with the real 3D structure, ET was applied using HAADF-STEM mode. The sample was prepared using a Dual Beam FIB/SEM. For that purpose, the Fe_2O_3/PE rods were first mounted on a pin mount SEM specimen holder using a silver paste. Thin layer of platinum was then deposited in vacuum onto the surface to prevent surface charges during imaging and FIB operations. Figure 12(a) shows the annular shaped ion milled area around the specimen pillar and a box milled for direct view during cutting of the pillar. The specimen was brought to TEM grid with an omniprobe (figure 12(b)) and

milled further with annular patterns. The final polishing was done using low ion currents and the final structure as used in ET is shown in figure 12(c).

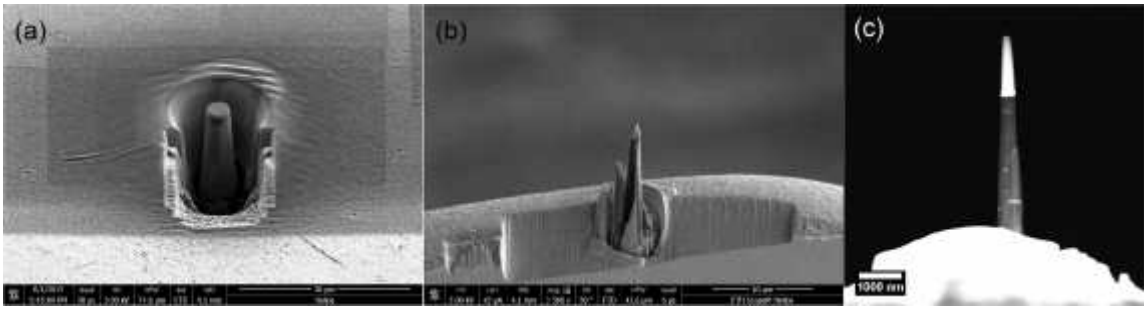

Figure 12 (a) SEM image of the annular milling pattern around the pillar specimen. (b) SEM image of the pillar after transfer to TEM grid and rough polishing (c) HAADF-STEM image of the final polished structure for ET. The bright peak of the pillar is an IBID platinum protection layer.

Tilt series were acquired with FEI Talos, operated at 200 kV. The tilt angles ranged from -78° to 78° with 2° increments. Figure 13(a) shows the zero degree HAADF-STEM image. The tilt series was aligned with IMOD program using the Fe_2O_3 nanoparticles as fiducial markers. Reconstruction was done the Digital Micrograph environment using SIRT with 10 iterations. Avizo program was used to filter the reconstruction with non-local means filter and segmented first automatically using global threshold and then using final manual adjustments. One 2D plane of the reconstruction and its segmentation results can be seen in figure 13(b). A volume rendered visualization of the 3D structure acquired from the segmentation is shown in figure 13(c).

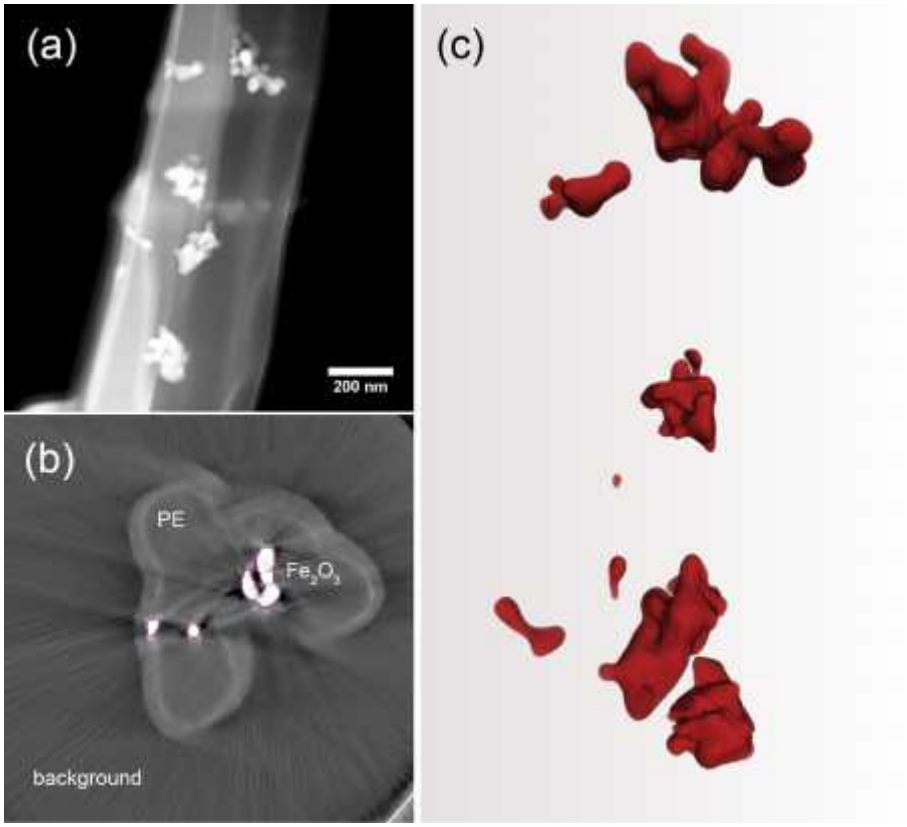

Figure 13 (a) Zero tilt HAADF-STEM image from the acquired tilt series. (b) 2D Reconstruction showing the segmentation results. (c) Volume rendered 3D image of the iron oxide agglomerates.

4.4.2 2D/3D Comparison

By comparing the triangulated surfaces of the Fe_2O_3 agglomerates in figure 14 to their 2D zero tilt HAADF-STEM images with segmentation results, it is clear that a 2D segmentation of a projected complex 3D agglomerate is prone to mistakes. ET unravels the lost projected dimension of the agglomerates but due the extreme complexity of the structure, it is even then hard to determine the primary particles within the agglomerate. The left images in figure 14 are positioned approximately at the same position as the zero degree projection. And the right ones are rotated vertically approximately 150° degrees. Even with the simplest particle in figure 14(b), it is challenging to resolve primary constituents. In figure 14(c), the rotated image shows, that all these upper separate particles are marked by just one particle in the 2D segmentation. The 2D segmentation results for the sizes of the primary particles in figure 14(d) are completely arbitrary. It is thus concluded that complementary techniques have to be considered to resolve the PSD of primary particles of highly complex agglomerates.

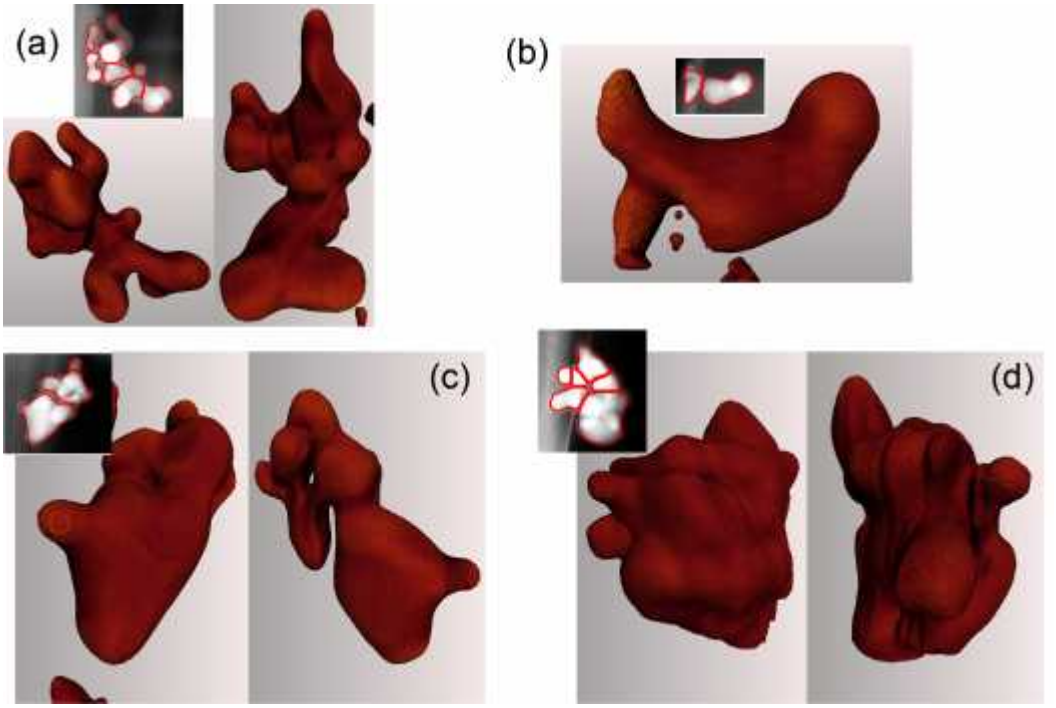

Figure 14 2D segmentation results as compared to the real 3D structure of the iron oxide agglomerates, visualized as triangular surfaces. The right most images are rotated clockwise about 150° degrees vertically from the left images.

The NanoDefine Particle sizer has an option for single particle mode, where agglomerates are not included by using a high convexity threshold value. This way, all the above mentioned challenges are avoided. Less particles will be detected but this can be compensated by acquiring more images. The PSD analysis with single particle mode is shown in figure 15. It is evident from the image, that no agglomerates were included. A median value of 38.8 nm was obtained, which is surprisingly larger than the one acquired from a PSD in figure 11. This apparent inconsistency is most likely due to erroneous splitting of the agglomerates into primary constituents. Using only single particles as well as very clearly separable primary constituents attached to an agglomerate, more accurate and trustworthy PSDs can be achieved in a fully automatic mode.

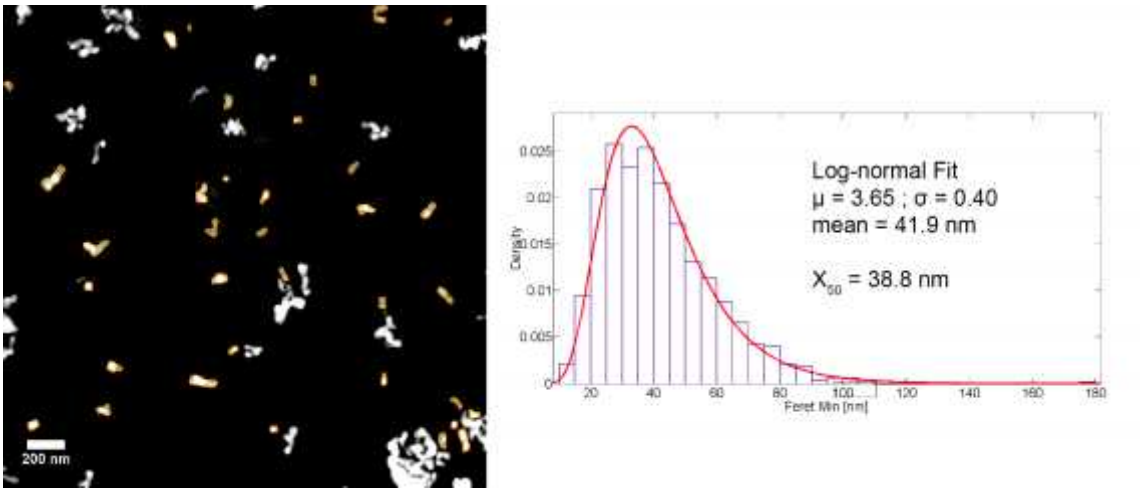

Figure 15 HAADF-STEM image of the hematite NPs with segmentation results using single particle

mode. On the right a PSD with mean and median values. N = 1039.

5 TiO_2 in Sunscreen (semisolid matrix)

This chapter focuses on sample preparation methods for TiO_2 in sunscreen for EM characterization needs.

5.1 Direct Observation of Nanoparticles from Cosmetics

Three electron microscopy approaches, WET-SEM (Scanning Electron Microscopy of environmental cell), cryo-(FEG-)SEM (Scanning Electron Microscopy at low temperature), and WET-STEM (Scanning Transmission Electron Microscopy under hydrated condition in an Environmental Scanning Electron Microscope *ESEM*), have been investigated on simple formulas, very similar to ID 13b, and containing the exact same nano-TiO_2. In WET-SEM, 15µl of sunscreen is deposed in a hermetic environmental capsule (Quantomix QX). The sealed capsule is then mounted on the microscope stage, and observation takes place through a membrane transparent to electrons using a BSE detector in a tungsten emission Variable Pressure Hitachi S3400N SEM. Under these conditions, individual nanoparticles cannot be identified; agglomerates/aggregates can be observed (Figure 16). Moreover, Quantomix environmental cell has the disadvantage of allowing only the observation of particles that are in direct contact with the membrane. It is possible that images obtained do not represent the real particle distribution. Also, the fact that ultimate resolution cannot be reached impairs nanoparticle identification.

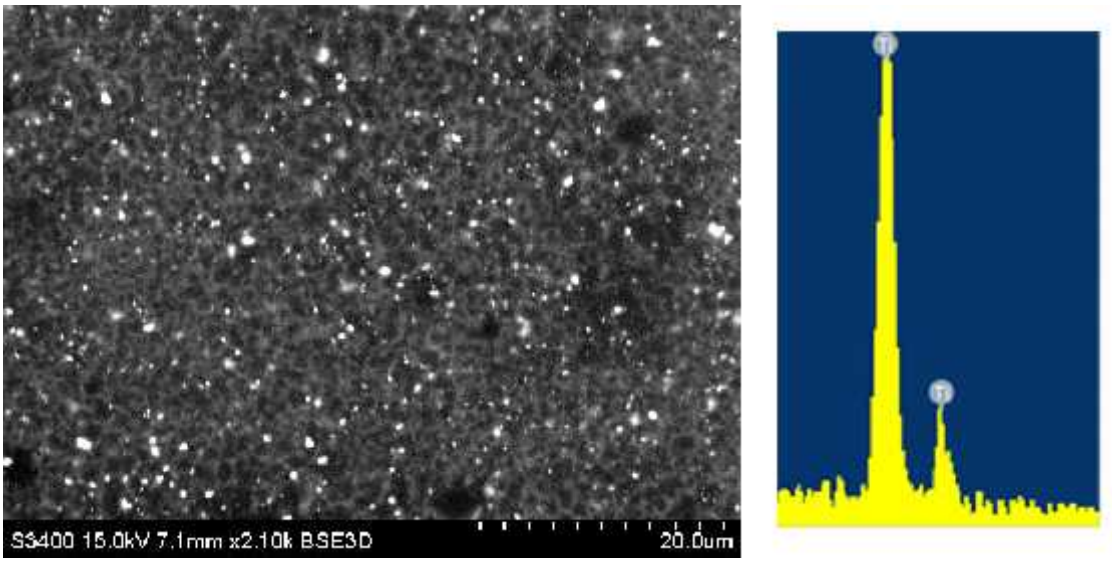

Figure 16 WET-SEM (Quantomix cell): In the limit of our study, this technique gives an overview of agglomerates/aggregates distribution, EDS can be conducted on sample (right). However, individual nanoparticles could not be identified (BSE image).

For cryo-SEM observation, we use the same quantity (15µl) of finished product which is squeezed between two graphite stubs (Pelco graphite mount 15 mm and graphite mount 25 mm). Conductivity and low atomic number are favourable for both a rapid freezing and artefact free observation and analysis. The sandwich is then fast frozen in Nitrogen slush (VG system) and subsequently transferred onto the cold stage of the scanning electron microscope (Hitachi S3400N), opened, quickly placed under low vacuum and maintained at Low temperature (-50°C) on a Deben Peltier Stage during observation. A controlled pressure (from 6Pa to 60Pa) is maintained in the microscope chamber in order to neutralize residual electric charges. Under these conditions, individual nanoparticles can be identified in the sunscreen (Figure 17). The hydration state of the sample is not stable during observation under the chosen conditions of pressure and temperature, and a freeze-drying process occurs that can in fact be beneficial to the analysis. However, although Ti is clearly associated with agglomerates/aggregates (Figure 18), analytical resolution is not sufficient for EDS individual particle analysis. Cryo-FEG-SEM (Cryo Field-Emission Gun Scanning Electron Microscopy; Jeol 6300F) has also been previously applied to a simple formula. After slam-freezing at liquid helium temperature (Ultra-Freeze MF 7000 from RMC), observations of cryo-fractures of the sample were conducted in the FEG-SEM at -180°C. Individual crystals of nano-TiO_2 could be resolved.

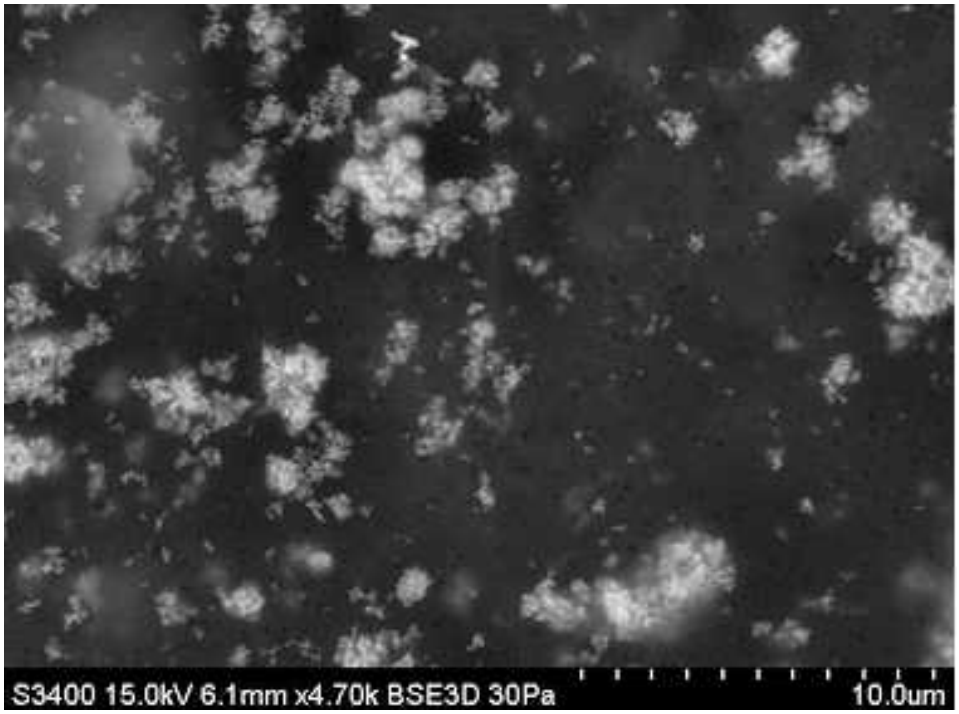

Figure 17 Cryo-SEM in a Variable Pressure SEM (tungsten emission) : from observation of graphite stub at low temperature, individual nanoparticles can be identified in sunscreen (BSE image).

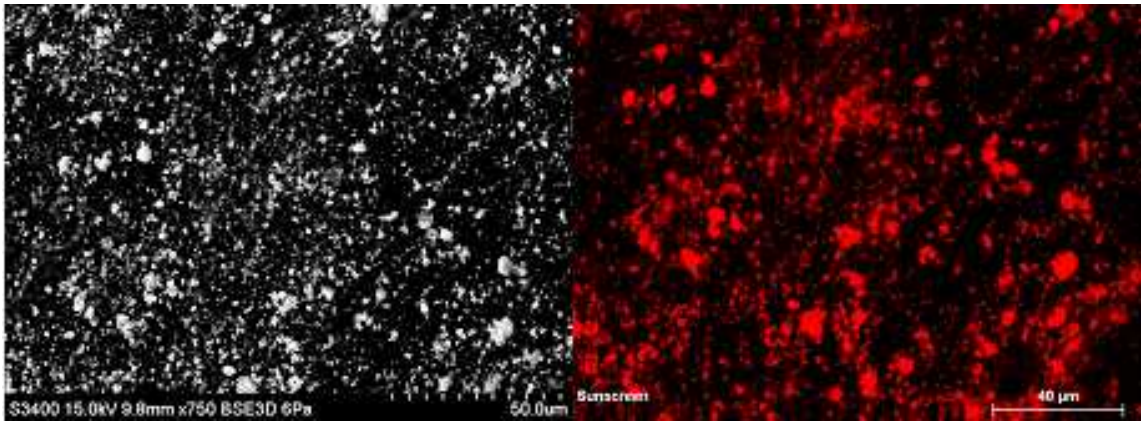

Figure 18 Low magnification: Energy Dispersive Spectrometry (EDS) Titanium mapping on the sunscreen (right) from the BSE image on left (Ti Kα).

In WET-STEM, a small quantity of sunscreen is deposed on a TEM carbon-Formvar grid (Pelco pure carbon 200 meshes) and removal of product in excess conducted in order to obtain a micrometer range thick layer of sunscreen over the grid. The TEM grid is then observed under environmental conditions in STEM mode in a Quanta 400 FEI ESEM. Nano-TiO_2 particles can be clearly identified in figure 19. However, because the higher the humidity, the lower the resolution, best compromises in terms of temperature/pressure were evaluated. In figure 20, we can appreciate the gain in contrast and resolution when the humidity in the microscope chamber varies from high humidity to high vacuum. Although further studies have to be conducted, one can note that, during this slow drying of the sample, particle distribution seems to remain stable, i.e. no agglomerate or aggregate formation can be observed.

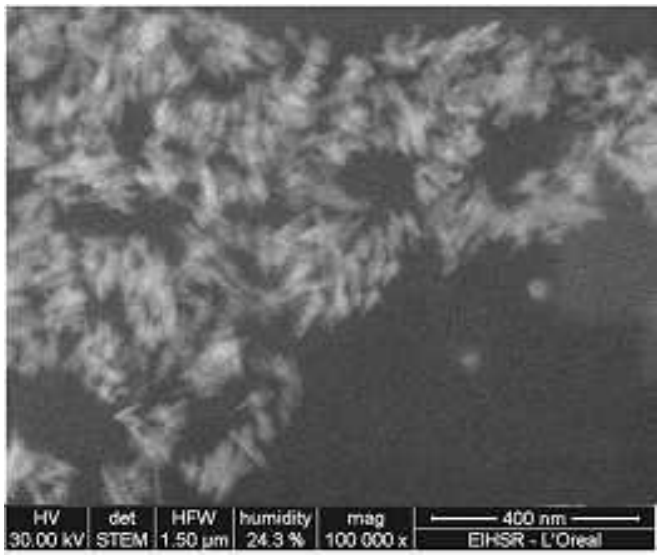

Figure 19 WET-STEM mode in a Quanta 400 FEI ESEM, nano-TiO_2 particles are clearly identified on this WET-STEM image acquired at 24% humidity.

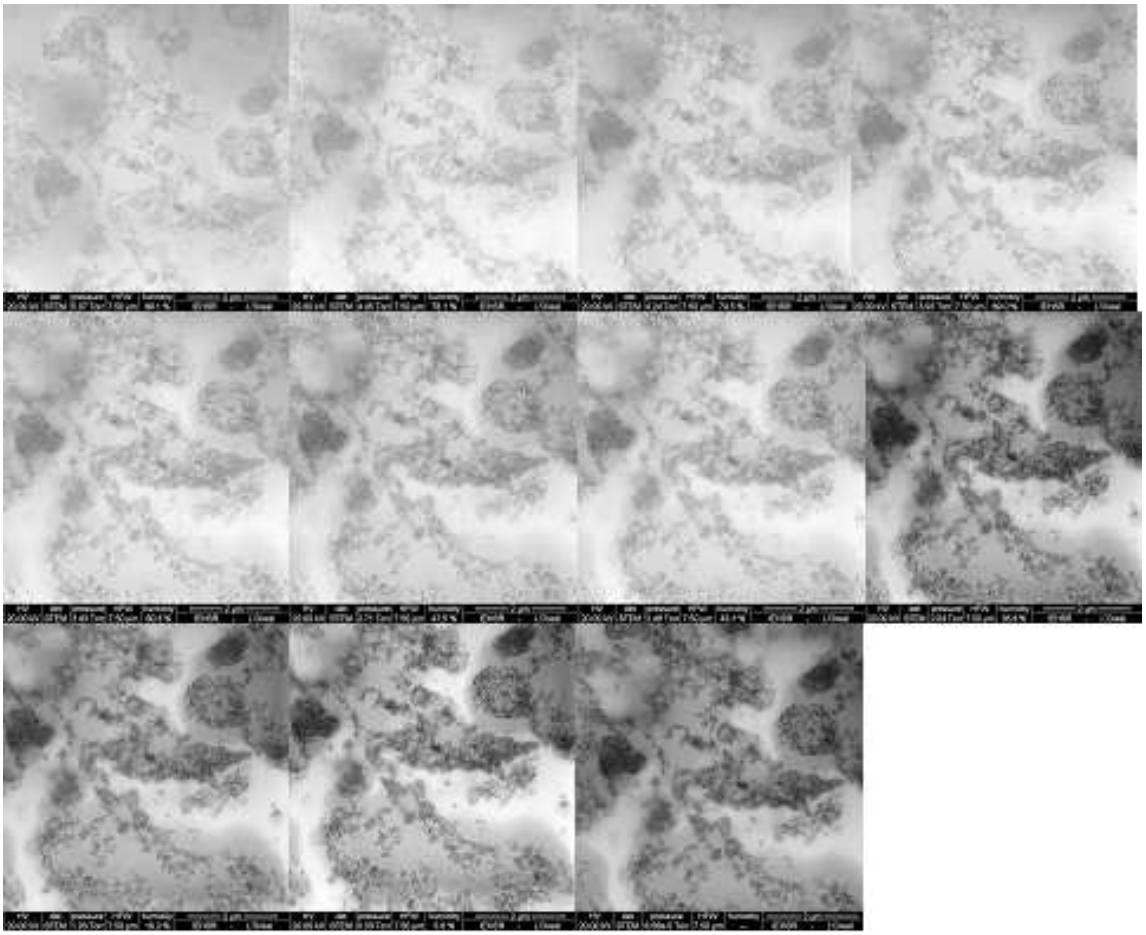

Figure 20 Images obtained from RH89% (WET-STEM, upper left image) to high vacuum conditions

(STEM, same detector, lower right image). No agglomeration occurred during the process.

Preliminary results obtained from cryo-TEM on isolated TiO_2 nanoparticles (deposition of 7 µl of an aqueous suspension on a glow discharge pretraited carbon coated TEM grid and subsequent plunge freezing in liquid ethane) in a FEG JEOL 200kV energy filtered microscope preclude a direct application to finish products. In fact, film thickness required for image acquisition in low electron dose mode is limited to an incompatible maximum of 100 to 200 nm.

Finally, WET-STEM seems the best candidate for a direct detection of nanoparticles in finished product, although it has to be evaluated with smaller and less electron dense material. However, given the complexity of cosmetics, it cannot be readily applied to particle counting.

5.2 Extraction and Analyses of TiO_2 in Cosmetics

Although allowing the detection of nanoparticles, direct observation of finished product by EM does not readily give access to particle size distribution. To circumvent this limitation, extraction of particles from the organic matrix, prior to the determination of particle size distribution, by means of EM or other techniques, has been investigated.Three samples were delivered to the ND consortium:*i* ID 13a is the actual representative sample, containing 4% NanoTiO2, with an aluminum salt based surface treatment, as a UV filter, plus: micro-Titanium and Iron oxides for coloring purpose;*ii* ID 13b, is a simplified formula, containing 4% NanoTiO2, with an aluminum salt based surface treatment, as a UV filter (same particles as for ID 13a); *iii* A blank formula, without mineral particles (noted ID blank) has been provided. ID 13b and ID blank were delivered to the Consortium for the purpose of helping for the extraction of Nano-particles from ID 13a. The organic components are identical for the three samples. Extraction protocols using solvents and using thermal treatments have been investigated.

5.2.1 Extraction of Particles using Solvents

Protocols for the extraction of particles using ethanol and centrifugation are detailed in appendix B.

5.2.1.1 Ethanol and Centrifugation

The insoluble fractions have been weighted for the three products, and corresponding percentage determined in mass:

ID 13a: the insoluble fraction corresponds to **11.1%** of the initial formula

ID 13b: the insoluble fraction corresponds to **7.7%** of the initial formula

ID blank (blank formula): the insoluble fraction corresponds to **3.3%** of the initial formula

When performed on initial formula 13a, EDS in an ESEM demonstrated a ratio Ti Kα/Fe Kα of 3.85 (Figure 21), comparable, considering matrix effects, to the ratio of 3.43 obtained from the insoluble fraction of ID 13a (Figure 22).

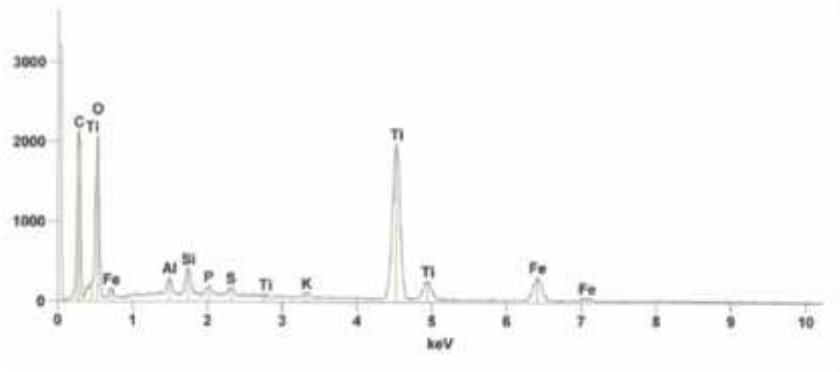

Figure 21 EDS signal from initial product 13a.

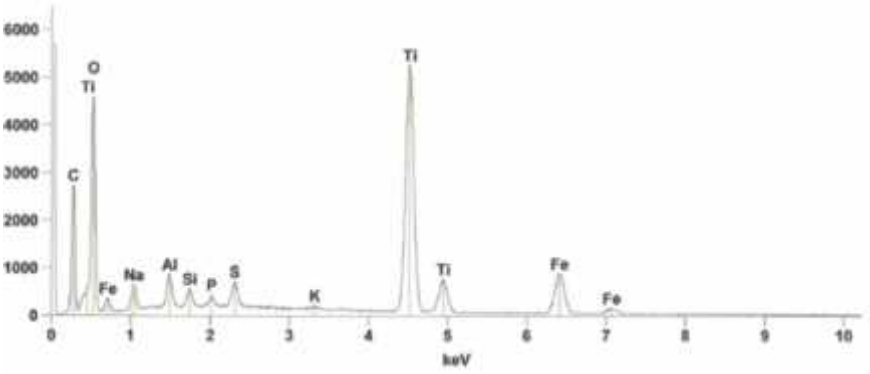

Figure 22 EDS signal from the insoluble fraction extracted from 13a.

The complete formula ID 13a:

After dispersion, particle sizing has been performed using SLS (static light scattering) with a Mastersizer 3000 from Malvern.

Dispersion: 1% w/w of solid residue in 1% w/w surfactant solution (sodium dodecyl sulfate) using vortex mixer; magnetic stirrer and ultrasonic bath. Results are shown in figure 23 and figure 24.

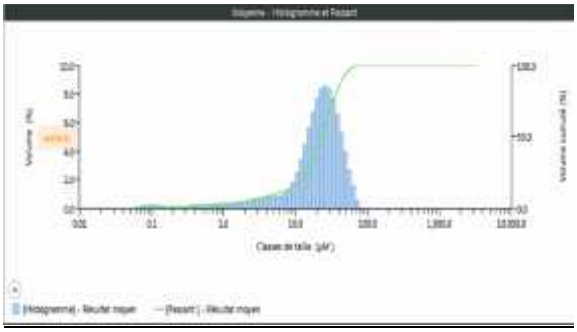

Figure 23 ID 13a Particle sizing by SLS (size distribution by volume).

D10: 5.10µm / D50: 22.04µm / D90: 44.30µm

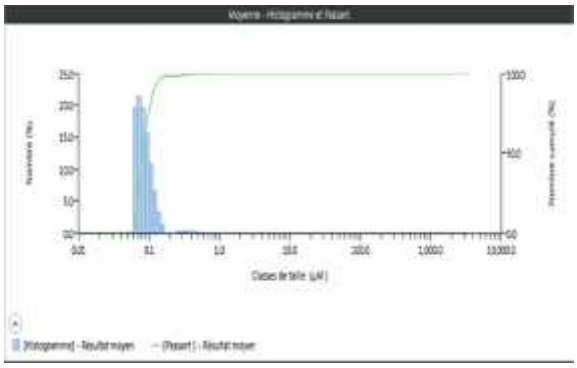

Figure 24 ID 13a Particle sizing by SLS (size distribution by number).

D10: 0.06µm / D50: 0.08µm / D90: 0.12µm

The population of nanoparticles can be identified from the particle size distribution in figure 23, and more clearly in figure 24. Residues have also been observed by TEM (Figure 25), which shows TiO_2 nanoparticles, non-nano round particles (possibly TiO_2) and non-nano rods (possibly iron oxide).

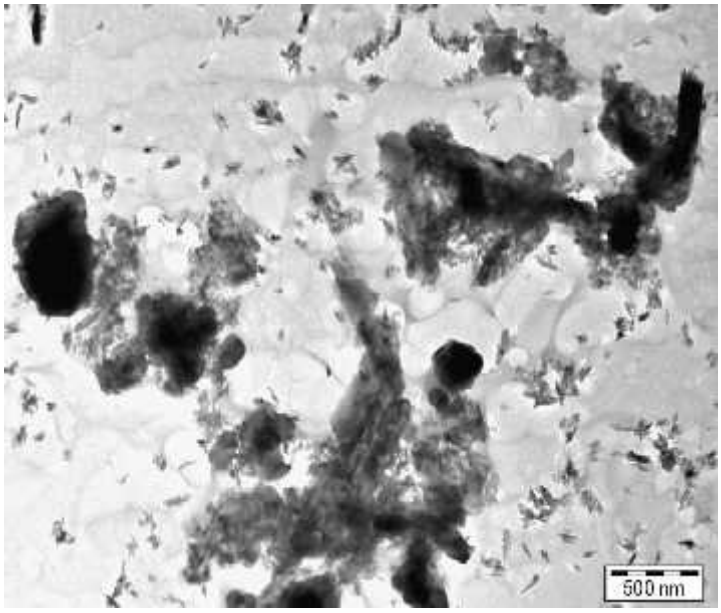

Figure 25 TEM image of the dispersion of the insoluble fraction (ID-13a).

The simple formula ID 13b:

The TEM microphotography in figure 26 shows small agglomerates/aggregates of TiO_2 nanoparticles.

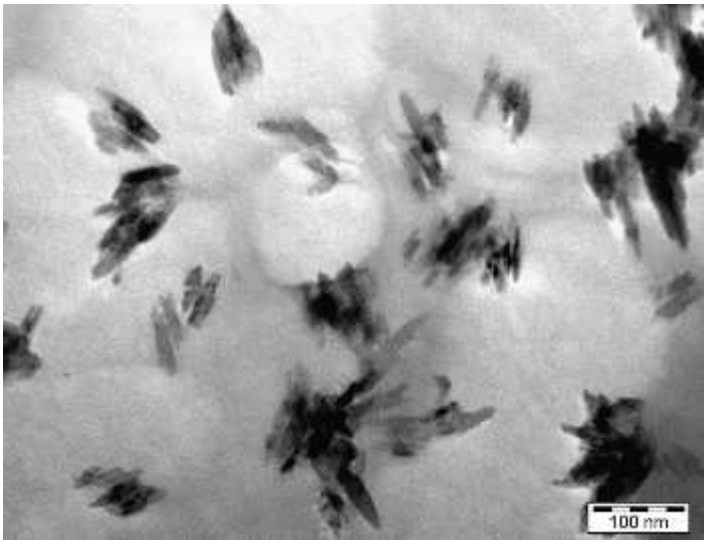

Figure 26 TEM image of the dispersion of the insoluble fraction (ID-13b).

5.2.1.2 Toluene and Ethanol using Sohxlet Apparatus

1 g of sample and 100 ml of solvent are used. Sample is enclosed into a PTFE filter and maintained in the extraction thimble. 10 cycles of solvent/Soxhlet (Figure 27) evaporation are applied, at a temperature of 110.6°C.

Figure 27 A Soxhlet apparatus used in this protocol.

With toluene, the insoluble extract corresponds to **26.6%**, **14.4%** and **15.3%** for ID 13a (complete formula), 13b (simple formula) and blank (blank formula), respectively.

With ethanol, the insoluble extract corresponds to **11.8%, 8.4%** and **3.9%** for ID 13a (complete formula), 13b (simple formula) and blank (blank formula), respectively.

Ratios Ti Kα/Fe Kα of 6.91 (Figure 28) and 1.46 (Figure 29) have been obtained (EDS in an ESEM) from the insoluble fractions of ID 13a after respectively toluene/Soxhlet and ethanol/Soxhlet extractions.

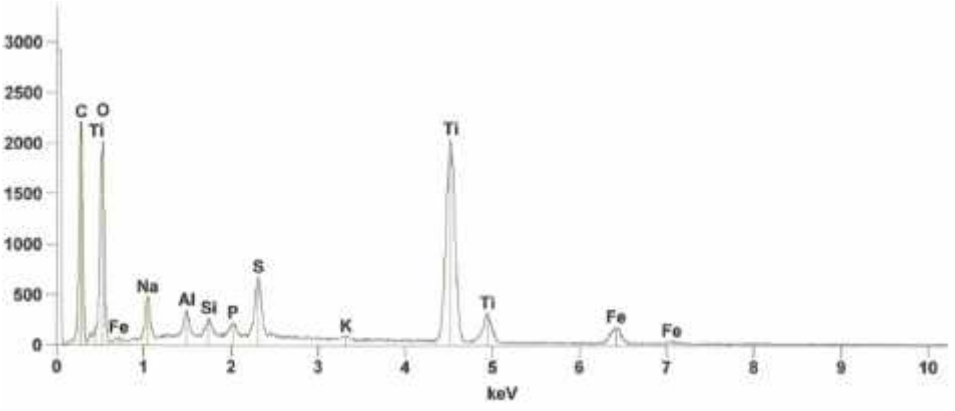

Figure 28 EDS from the insoluble fraction extracted from 13a using toluene/Soxhlet protocol.

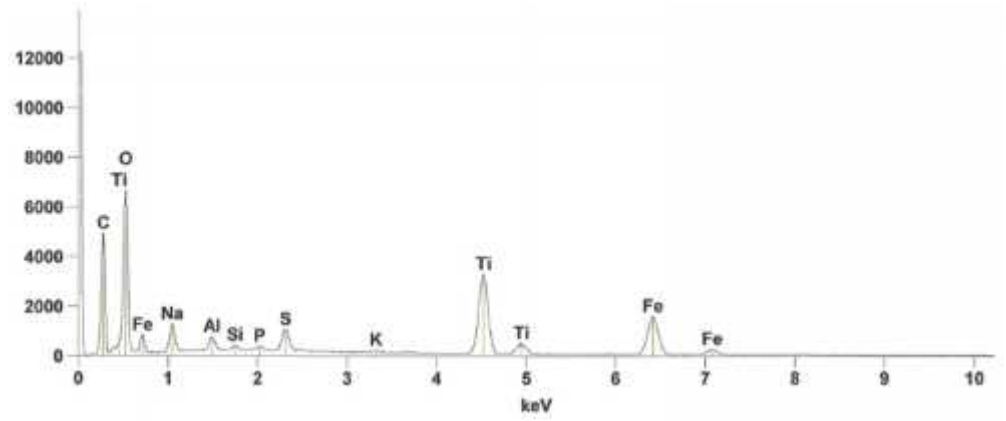

Figure 29 EDS from the insoluble fraction extracted from 13a using ethanol/Soxhlet protocol.

When compared to Soxhlet, extraction using centrifugation and ethanol gives the lowest percent of insoluble fraction. It is assumed that the protocol removes the organic phase and that the correct protocol should give a close to zero % residue from the blank formula and a 4% mineral residue from ID 13b. Percentages obtained, together with EDS ratios, are in favor of the ethanol/centrifugation protocol.

When ethanol/Soxhlet or toluene/Soxhlet insoluble fractions are observed by TEM, mineral particles can also be identified. However, the aspect of agglomerates/aggregates (Figures 25, 26 and 30 to 35) and EDS counting (Figures 21, 22, 28 and 29) together with the percentages of insoluble fractions corresponding to different methods, are strongly in favor of the ethanol/centrifugation protocol for subsequent counting.

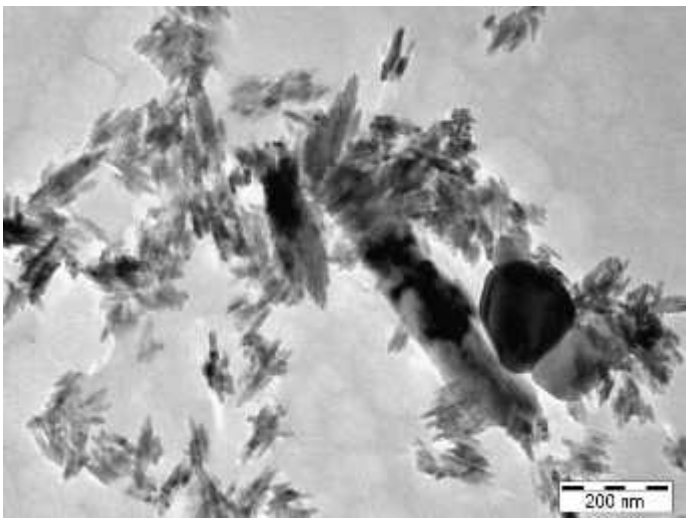

Figure 30 TEM image of the insoluble fractions, ethanol/Soxhlet ID 13a (complete formula).

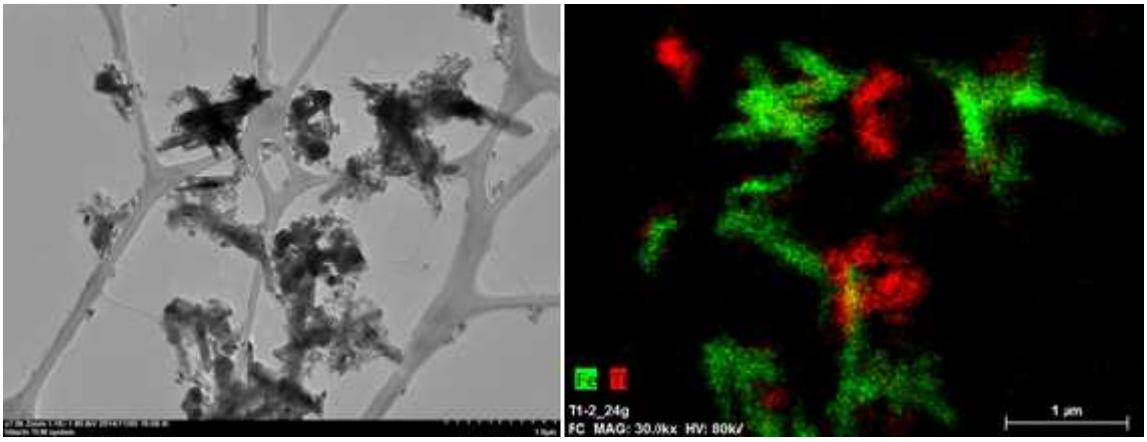

Figure 31 TEM image of the insoluble fractions, ethanol/Soxhlet ID 13a and corresponding EDS.

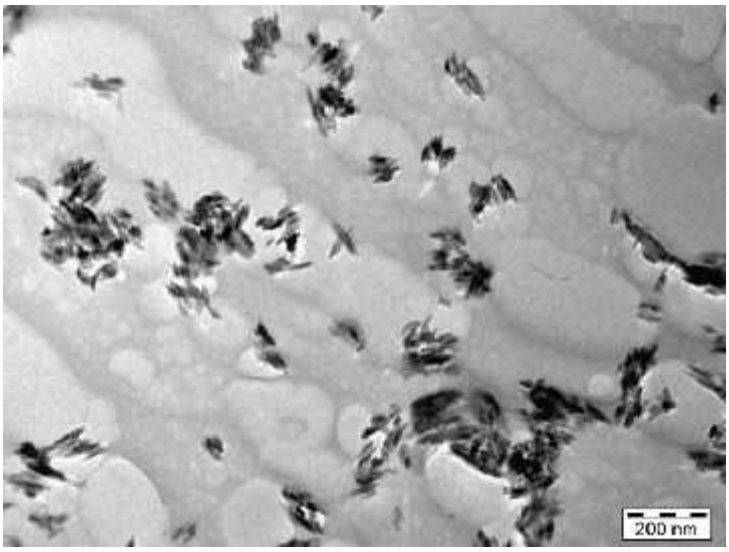

Figure 32 TEM image of the insoluble fractions, ethanol/Soxhlet ID 13b (simple formula).

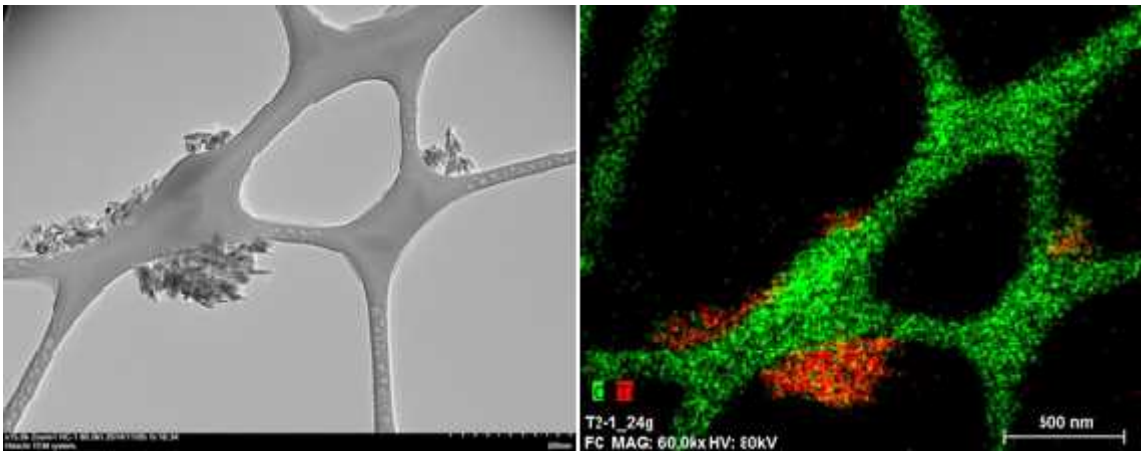

Figure 33 TEM image of the insoluble fractions, ethanol/Soxhlet ID 13b and corresponding EDS map. (Titanium in red, Carbon from the support lacey film in green).

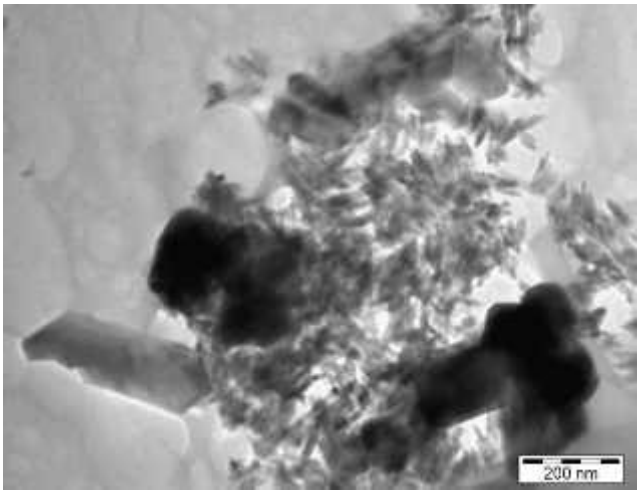

Figure 34 TEM image of the insoluble fractions, toluene/Soxhlet ID 13a (complete formula).

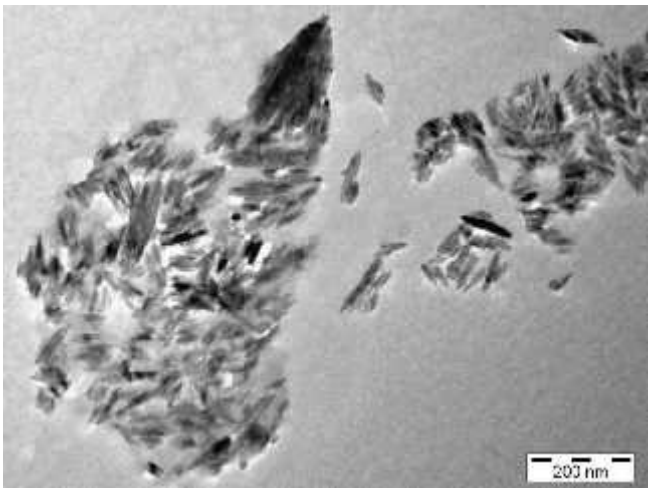

Figure 35 TEM image of the insoluble fractions, toluene/Soxhlet ID 13b (simple formula).

Based on these results, we recommend to use the ethanol/centrifugation procedure. This protocol does not impose a limit on the quantity used for extraction (in these study, we used 5g of formula). On the contrary Soxhlet can only process 1 g of formula (in two hours). However, one advantage of the Soxhlet is the limited human intervention in the process

5.2.1.3 Solvent for Mass Residue Dissolvent

One could expect a close to zero % insoluble residue from the blank formula. In fact the residue corresponds to 3.3 % of the initial mass of product used. The arising question was: How could we improve the process? Hence, a protocol was developed to dissolve the residue from the ethanol/centrifugation protocol.

Protocol developed:

- On 10mg of residue, add solvent: final concentration 2.5mg for 1ml of solvent.
- Ultrasonic bath during 15min (measured temperature varied from 25°C to 35°C)
- After 24h at room temperature: optical observation of the residual precipitate.

Several solvents of different polarities have been investigated, together with a strong acid (HCL) and a strong base (NaOH) solutions.

Solvents tested and conditions:

Water (35°C) (90°C); NaOH (50%) (35°C); HCL (0.5N) (25°C); Methanol (35°C); DMSO (35°C) (90°C); Acetone (35°C); Ethanol (35°C); Ethyl Acetate (35°C); THF (35°C); Dichloromethane (35°C); Toluene (35°C); Heptane (35°C).

Conclusion:

None of the solvent tested were able, in these operating conditions, to solubilize the residue obtained after the ethanol/centrifugation protocol.

Identification of the residue:

Infrared spectroscopy analysis was performed on the residue from ethanol/centrifugation protocol. Strong similarities exist between residue IR profile and modified starch IR profile (Figure 36). Aluminum starch octenylsuccinate is present in the formulas.

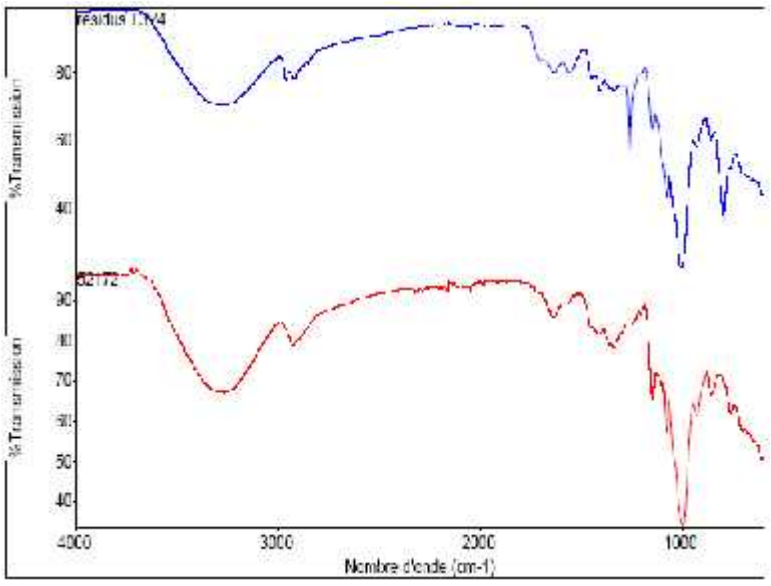

Figure 36 IR spectrum of ethanol/centrifugation residue (blue); IR spectrum of modified starch (red).

Particle sizing measurements (SLS: MS3000):

Particle sizing is performed after dispersion of the residue: Dispersion of 1% w/w of solid residue or aluminum starch octenylsuccinate sample in 1% w/w surfactant solution by using vortex mixer; magnetic stirrer and ultrasonic bath.

Particle size distribution of residue dispersion is similar to the distribution obtained from a dispersion of modified starch (Figure 37).

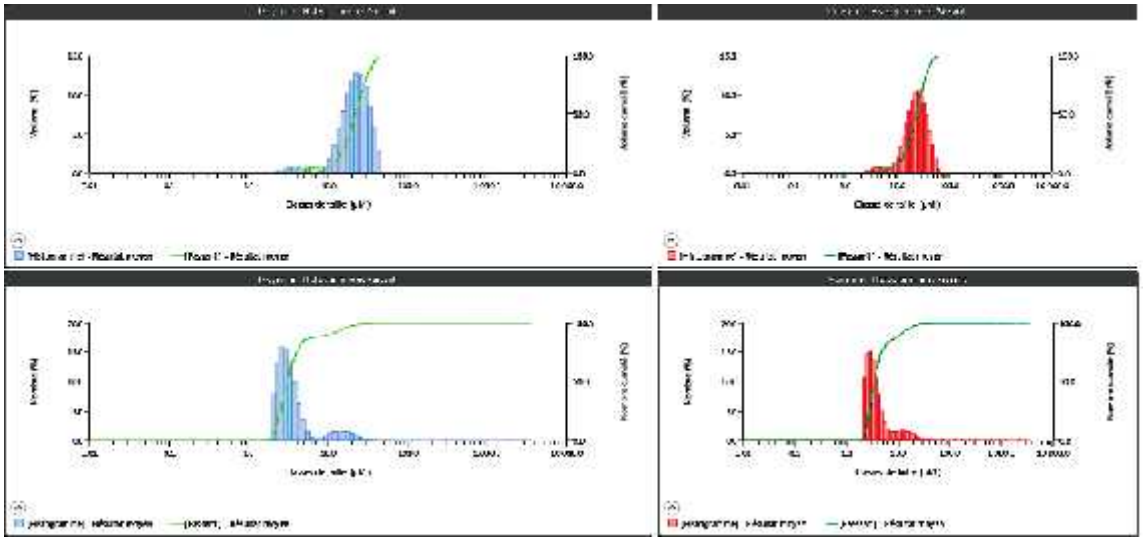

Figure 37 Distribution in volume (upper graphs) and number (lower graphs). In blue: residue from the blank formula, in red: modified starch.

Thermogravimetric analysis:

TGA (TGA7 from Perkin Elmer) of the residue from the blank formula is comparable to the TGA thermogram of the modified starch (Figure 38).

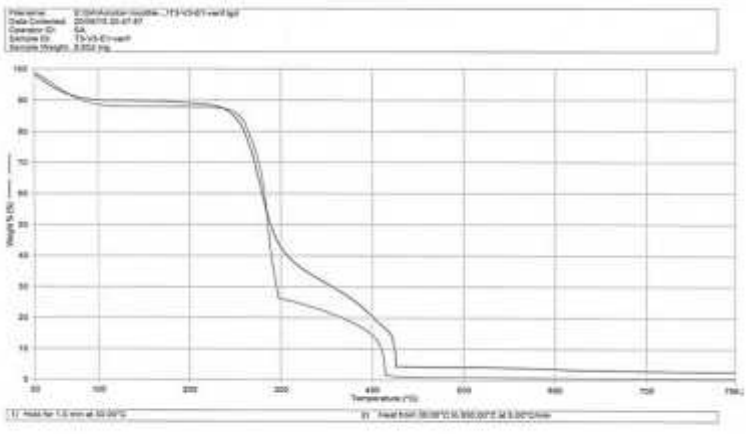

Figure 38 TGA thermogram from residue in blue and from modified starch in grey.

Dissolution of the residue:

A protocol aimed to dissolve polysaccharide (Polysaccharid Analysis, Ed Techniques de l'Ingénieur, Theo Efstathiou and Christian Nio, 10/03/2008) has been applied to the residue. Digestion with specific enzyme could also be considered.

5.2.2 Extraction of Particles using Thermal Degradation

The second approach explored to extract mineral particles was thermal degradation of organic components.

Thermogravimetric analysis:

Corresponding TGA thermograms are shown is Figures 39, 40 and 41.

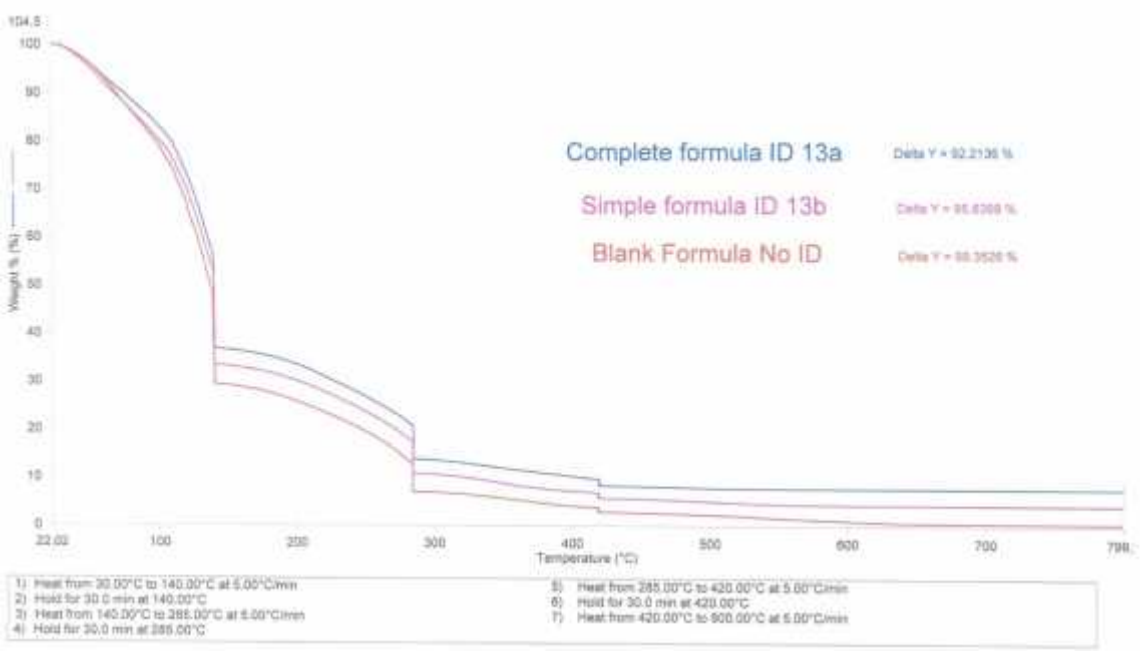

Figure 39 TGA curves from the three products (ID 13a; ID 13b; and ID blank (blank formula)). Heating from 30°C to 800°C at 5°C/min under air flow with three isothermal steps (30 min) at 140°C; 285°C; and 420°C.

The mass percentages of residues corresponding to Fig 39, are **7.6%**; **4.3%**; and **0.6%** for respectively ID 13a (complete formula), ID 13b (simple formula) and ID blank (blank formula = no mineral charges).

When compared to the mass percentages of residues after solvent extraction, a greater proportion of the organic matrix was removed (for example, data were for ethanol/centrifugation: 11.4%; 7.7%; 3.3% respectively).

Figure 40 shows the curves obtained without isotherms, the mass percentages of residues are in that case **7.6%**; **4.1%**; and **0.6%** for respectively ID 13a (complete formula), ID 13b (simple formula), ID blank (blank formula = no mineral charges).

These percentages are very similar to those obtained with isotherms. This last faster combustion process is therefore chosen for further experiments.

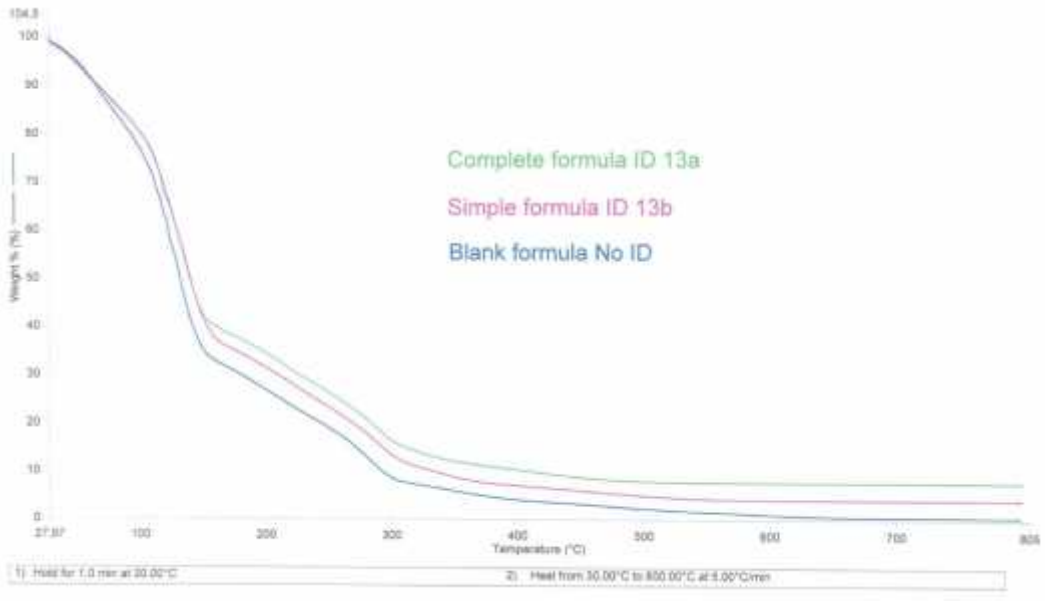

Figure 40 TGA diagrams for the three products, without isotherms.

In the case of Figure 40, mass percentages of residues were: Complete formula ID 13a, 7.6%; Simple formula ID 13b, 4.1%; Blank formula (ID blank): 0.6%.

On figure 41, we checked for the reproducibility of the measures, on product ID 13a (complete formula). The residues represent here 7.8±0.1% of the initial mass.

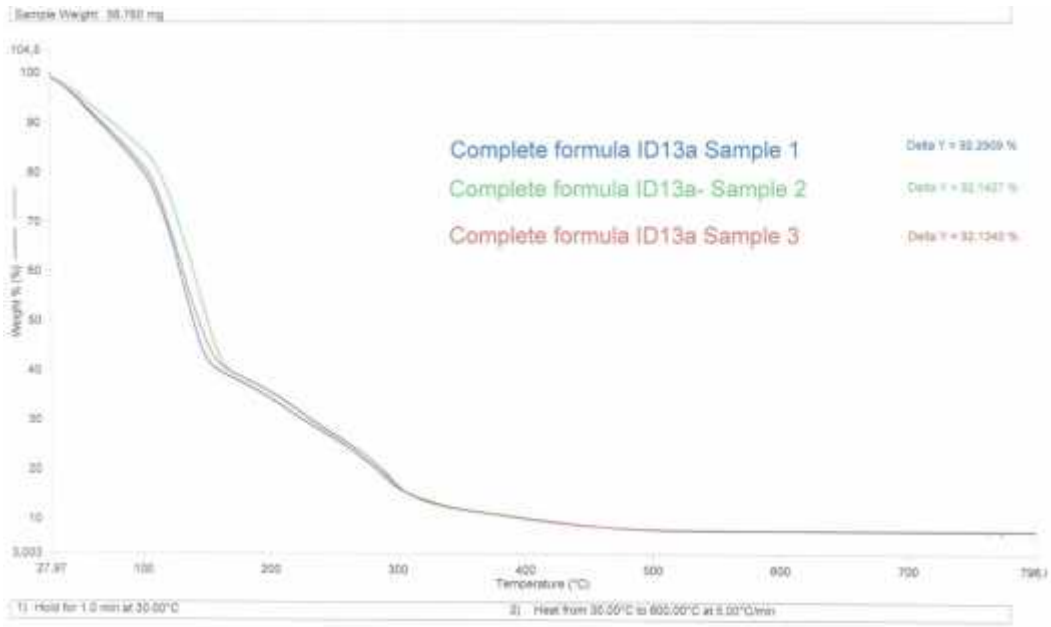

Figure 41 Reproducibility of the TGA measurements is demonstrated on three samples of product ID 13a.

SLS analysis:

The residue of ID 13a is dispersed in surfactant solution (Sodium Dodecyl Sulfate): Dispersion of 1% w/w of solid residue in 1% w/w surfactant solution using vortex mixer; magnetic stirrer and ultrasonic bath. SLS measurements were performed (Fig 42) and compared to ID 13a when using the ethanol/centrifugation protocol (Fig 43).

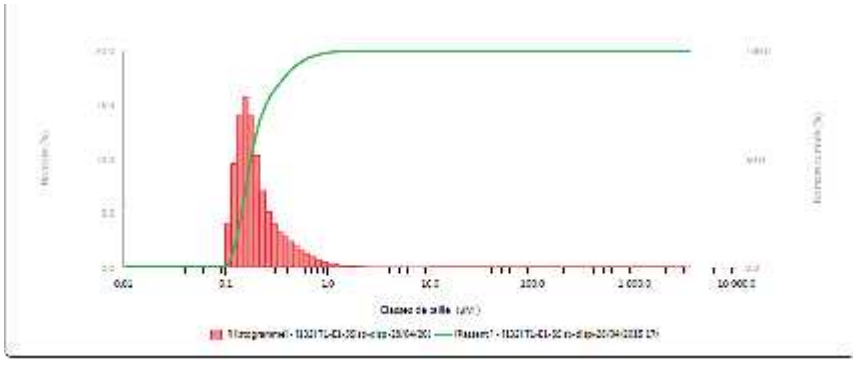

Figure 42 SLS particle sizing from the residue of product ID 13a obtained after thermic degradation (to be compared with Fig 43).

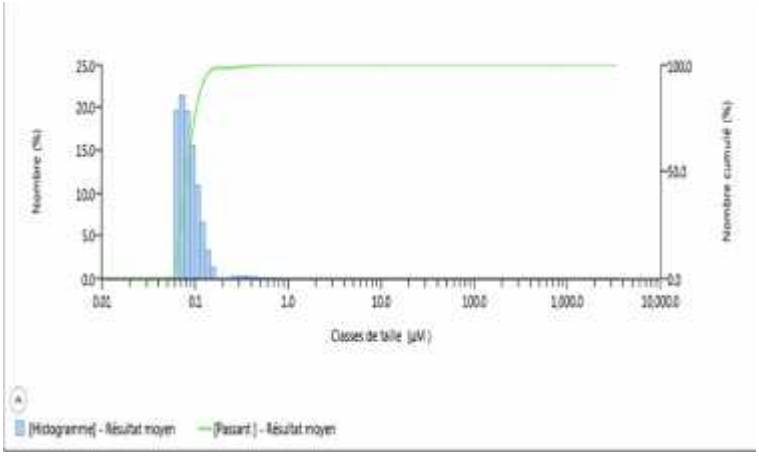

Figure 43 SLS particle sizing from the residue of product ID 13a obtained after ethanol/centrifugation protocol (to be compared with Fig 42).

A comparison of Figures 42 and 43 reveals an increase in particle sizes during the combustion process, compared to the ethanol/centrifugation process of particle extraction.

TEM/EDS analysis:

Figures 44 and 45 are respectively TEM images from residues obtained after combustion process and ethanol/centrifugation process, on ID 13a.

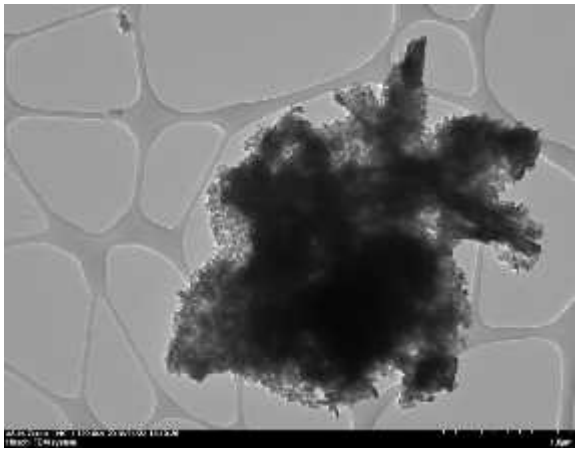

Figure 44 ID 13a, TEM image; residue from combustion.

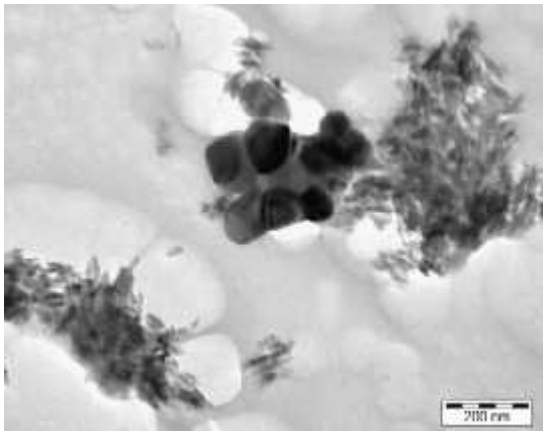

Figure 45 D 13a, TEM image; residue from ethanol/centrifugation.

A comparison of figures 44 and 45 reveals partial sintering between crystals on figure 44, whereas individual crystals are clearly observed after the ethanol/centrifugation process (Figure 45). These images are in agreement with particle sizing results.

Similar observations can be done from Fig 46 (ID 13b, thermal) and Fig 47 (ID 13b, ethanol/centrifugation).

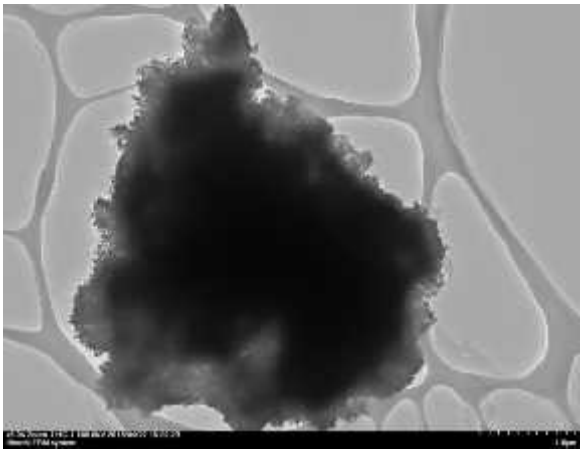

Figure 46 ID 13b TEM image, residue from combustion.

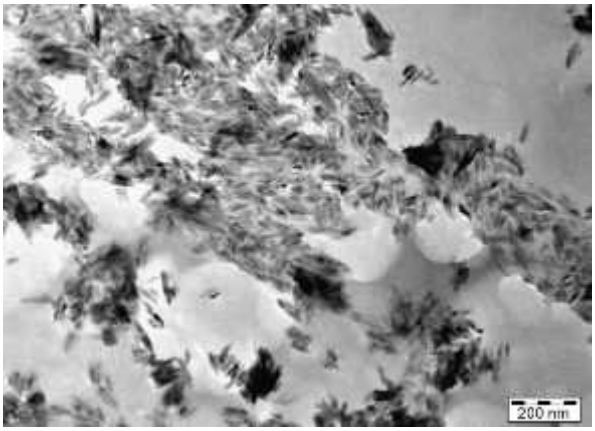

Figure 47 ID 13b TEM image, residue from ethanol/centrifugation.

EDS reveals Titanium and Iron are present in the agglomerates/aggregates observed after the combustion process (Figure 48 and 49).

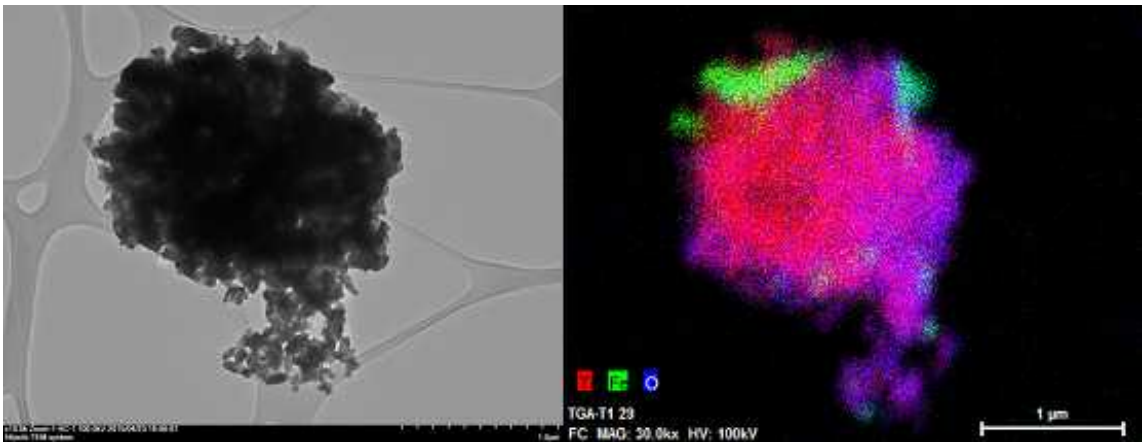

Figure 48 TEM image and EDS map of ID 13a. Detection of Ti and Fe in an agglomerate/aggregate of particles in a residue after thermal treatment.

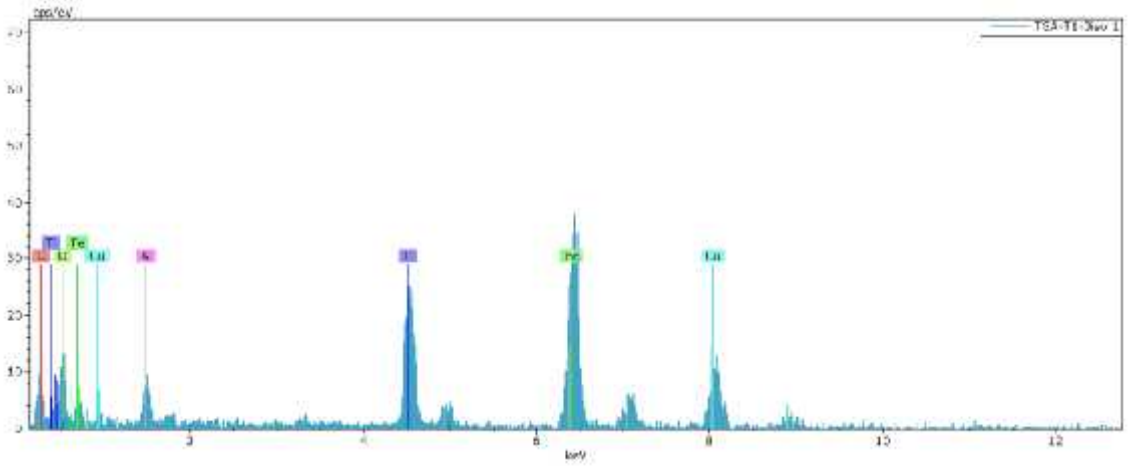

Figure 49 ID 13a EDS acquired from the green area of the agglomerate/aggregate of figure 48.

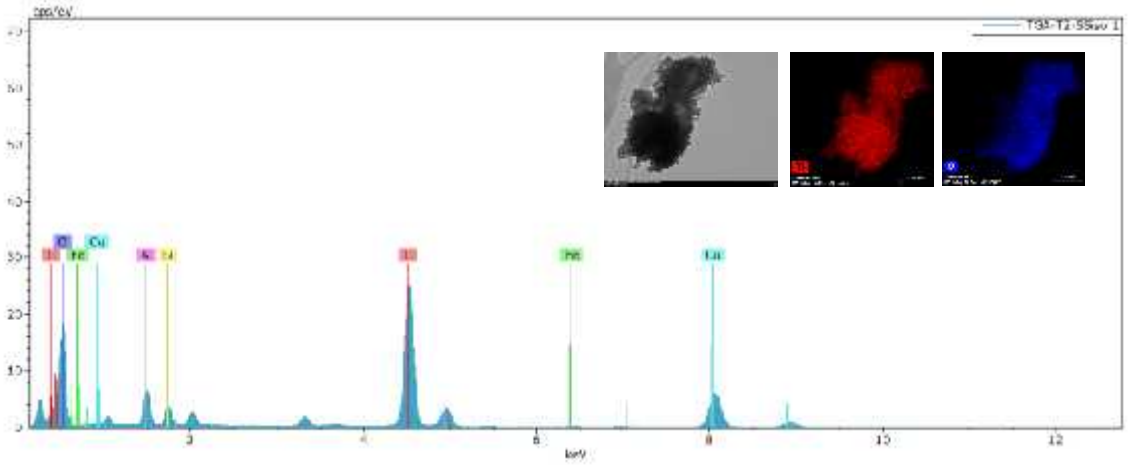

Figure 50 EDS acquired from agglomerates/aggregates of ID 13b after combustion.

Insets: Agglomerate/aggregate of nanoparticles contains Titanium (red) and Oxygen (blue).

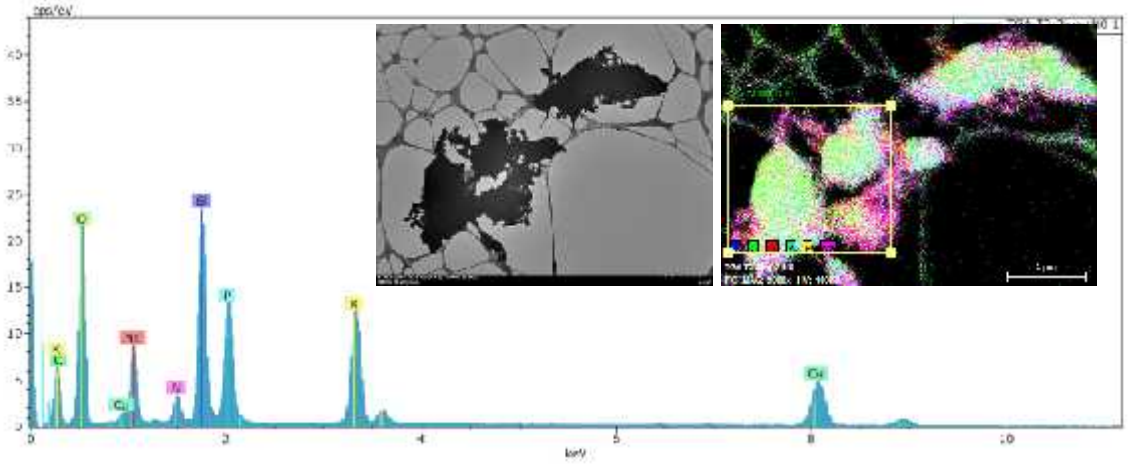

Figure 51 EDS spectrum acquired from residue of ID blank after combustion. Residue contains (EDS images) Carbon (green); Silicium (red); Potassium (light blue); Phosphorus (yellow); and Nitrogen element (pink).

Prospects:

A drawback of thermal treatment is clearly the observed aggregation/sintering of the material.

1) An attempt by lowering the maximum temperature to 400°C has been conducted (Figure 52), resulting in a higher mass percentage of residues, that are in that case **7.9%**; **6.0%**; and **1.7%** for respectively ID 13a (complete formula), ID 13b (simple formula), ID blank (blank formula = no mineral charges). These percentages have to be compared with figure 40. Deposits will be characterized by TEM and for particle sizing.

2) Another attempt was to thermally degrade the residue obtained after the ethanol/centrifugation protocol. Starting from 30°C up to 350°C with 1 long isotherm (600 min at 350°C) (Figure 53). Deposits have to be characterized by TEM and particle sizing.

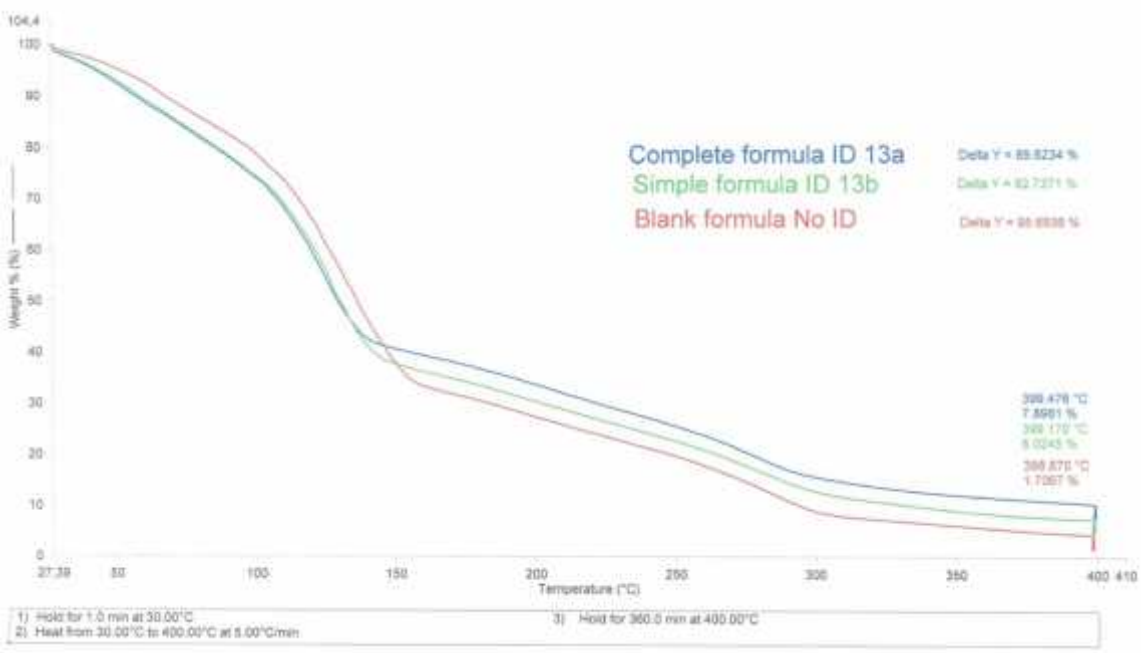

Figure 52 TGA curve acquired during heating from 30°C to 400°C at 5°C/min and Isotherm at 400°C during 350 min. Percentage of residues: Complete formula ID 13a: 7.9%; Simple formula ID 13b: 6.0%; Blank formula: 1.7%.

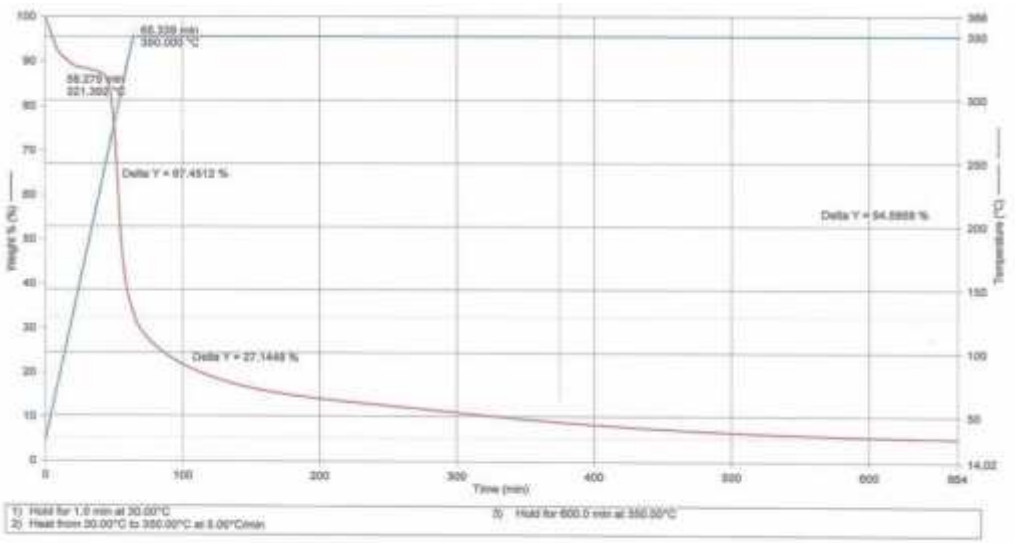

Figure 53 TGA curve acquired during heating from 30°C to 350°C at 5°C/min and Isotherm at 350°C during 600 min. Mass percentages of residue: 5.5% of the ethanol/centrifugation extract, i.e. 0.18% of the initial formula.

6 Conclusions

Applying thermal decomposition is the most straightforward method to extract the NPs from the PE matrix to determine the PSD. However this is possible only when the filler material has much lower melting point than the NPs and it is unclear how the treatment affects the NPs. Using FIB or UM it is possible to directly image the NPs within the PE with little or no risk to change the size or phase of the NPs. Soft materials like polymers tend to melt and bend under the FIB and thin enough lamellas are difficult to prepare. However for harder filler materials, this would be possible. Compression of the sections cut by UM results in difficulties in imaging conditions, such that at least fully automatic PSD analysis with no user bias is not straightforward. Applying low temperature heat treatment helps to straighten the PE sections that all NPs are in focus. For complex 3D NP agglomerates it was shown using ET, that the 2D segmentation results depends strongly on the projection dimension and gives incorrect results for the sizes of the NPs. Applying analysis using single particle mode ensures that only single and clearly separable particles are taken into account in the PSD.

Considering the results obtained from thermal degradation and solvent extraction, the best option for subsequent particle counting, by electron microscopy or other technique, is the ethanol/centrifugation process. A small proportion of organic matrix in the residue is still compatible with an observation by TEM and subsequent particle counting. In cosmetics, the mineral fraction will most often be composed of different types of particles, from nano-size particles to micro particles, in a usually rather complex organic matrix. Moreover, these particles are of different chemical compositions. If we take sample ID 13a, the complete formula, where a nano-Titanium dioxide (rutile) is used as UV filter, a non-nano Titanium dioxide (anatase) used for coloring purpose together with non-nano iron oxides, the challenge raises from the fact that if nanoparticles are detected under the TEM for example, their abundance in number will have to be associated to the non-nano fraction of the exact same type of particles. The fact that the mineral fraction is heterogeneous in terms of shape, size and composition imposes the use of separation and/or microanalytical techniques, in our case associated with diffraction techniques in order to discriminate between oxides. In conclusion, when nanoparticles are detected in a cosmetic formulation, identifying them as a nano or non-nanomaterial can be extremely challenging.

Appendix A Ultramicrotomy parameters

Figure 5(a): EAWAG

RT ultramicrotomy using a Leica EM UC6. The samples were embedded in epon block and trimmed to get a smooth cutting surface. Sections (70–120 nm) were cut with low speed 0.4 – 0.8 mm/min. The sections were left floating in water and transferred to TEM grid.

Figure 5(b): EAWAG

Cryo ultramicrotomy using a Leica EM UC6. Knife temperature -30°C and sample temperature -130°C. Sections were cut with low speed 0.4 – 0.8 mm/min. The procedure of BASF with DMSO and glycerine (75°C) was followed.

Figure 5(c): BASF

Cryo-ultramicrotomy using a Leica Ultracut EM UC7 (leica microsystems GmbH, Wetzlar, Germany) machine with -30°C knife temperature and sample temperature between -130°C and -140°C. Section thickness was varied between 70 nm and 120 nm. Samples were floated on a mixture of dimethyl sulfoxide (DMSO) and water. The samples were tempered afterwards in a glycerine bath at a temperature of approximately 60°C.

Figure 5(d): CODA-SERVA

The specimen is prepared by ultra-thin sectioning. After embedding in Epon medium, the specimen blocks are trimmed with a TM60 trimming unit to obtain a cutting face of 0.5 - 1 mm^2 to 1 - 2 mm^2. Ultrathin sections in the blue to green interference color range, corresponding with a section thickness between 150 - 250 nm, were cut with the Ultracut microtome and brought on pioloform-coated copper grids (200 mesh).

Appendix B SOP for Fe_2O_3 in Polyethylene Matrix

Standard Operating Procedure

Protocols for preparation of products for microscopy methods

Combined sample preparation and particle size distribution analysis of Fe_2O_3 nanoparticles in polyethylene

Version 1

1 Aim and Scope

The aim of this SOP is to provide and determine the sample preparation protocols and quantitative methods for fully automatic particle size distribution (PSD) analysis for Fe_2O_3 nanoparticles embedded in high density polyethylene (PE) matrix. The Fe_2O_3 in PE matrix was manufactured by industrial partners and, as received as small cylinder shaped rods. The dimensions of the rods were ~ 2 mm x 5 mm. The mass ratio of the hematite nanoparticles was 5% (g/g). The NPs were ~ 40 nm in diameter and were agglomerated into complex 3D structures.

This SOP describes the use of an ultramicrotome (Leica EM UC6) for sample preparation, a transmission electron microscope (TEM) operated in scanning mode (STEM, Hitachi HD-2700) for imaging and NanoDefine ParticleSizer for analysis. The scope of the sample preparation can be extended to any nanocomposite soft material that can be cut by an ultramicrotome; and the analysis guidelines are valid for any complex nanoparticle agglomerates.

2 Definitions

DF	Dark field
DMSO	Dimethyl sulfoxide
HAADF	High angle annular dark field
PE	Polyethylene
PSD	Particle size distribution
SOP	Standard operating procedure
STEM	Scanning TEM
TEM	Transmission electron microscope

3 Description

3.1 Materials and methods

Ultramicrotome: Leica EM UC6

Hotplate: Gerhardt Hotplate

TEM: Hitachi HD-2700 200kV

Software:

Digital Micrograph™ script for magnification calibration:
Find Cross grating distance
Online: http://portal.tugraz.at/portal/page/portal/felmi/DM-Script/DM-Script-Database

ImageJ plug-in for particle size distribution analysis:
Nanodefine ParticleSizer

Solvents for sample preparation:

MilliQ H_2O: Millipore Advantage A10
DMSO: Analysis Emsure® Acs from EMD Millipore

3.2 Performing measurements

3.2.1 Sample preparation

The Fe_2O_3 in PE rods were prepared using cryo ultramicrotomy (Leica EM UC6). The rods were first embedded in epon block and trimmed to get a smooth cutting surface. The diamond knife temperature was set to -30°C and sample temperature -130°C. Low cutting speed was applied 0.4 – 0.8 mm/min. The sections were left floating in a mixture of H_2O/DMSO at 75°C and then transferred to TEM grids. This procedure results in crushed sections with a wavy structure. The TEM grids were then placed on top of a clean pin mount SEM holder and heated (Gerhardt Hotplate) for 1h at 120°C to straighten the sections.

3.2.2 Measurement description

The most prominent TEM calibration related to PSD analysis is the magnification calibration. This was done using a standard cross grating sample and a custom written automatic software (Find cross grating distance) for the pixel size calculation. The eucentric height has to be accurately determined such that no large defocus deviation occurs. The microscope should be additionally well aligned (user alignments) for optimized imaging conditions. Dark field (DF) or high angle annular dark field (HAADF) mode is recommended. The magnification should be chosen such that the smallest estimated particles are at least 10 pixels across (here at least 40 kX). The number of images should be chosen such that the PSD contains at least 1000 particles.

3.3 Evaluation of results

Due to the complex 3D structure of the agglomerates it is recommended to use single particle mode of the NanoDefine ParticleSizer and irregular watershed with high convexity threshold (> 0.9). All images should be visually checked and possible agglomerates should be removed. Figure 15 gives an example of a segmented HAADF-STEM image (20 images in total) with final PSD using the Feret Min as a respective measurand. The total number of particles was 1039. The PSD was fitted using a log-normal curve with X_{50} = 38.8 nm.

4 Validation status

This method is not yet validated.

5 HSE issues

DMSO:

Flammable liquid and vapour. Keep away from hot surface, sparks and other ignition sources. Take precautionary measures against static discharge. Wear protective latex gloves, protective clothing, eyes and face protection.

TEM:

The user should be trained and guided to proper and safe usage of a TEM.

Ultramicrotome:

The user should be trained and guided to proper and safe usage of an ultramicrotome.

Appendix C SOP for TiO_2 in Sunscreen

Standard Operating Procedure

Protocols for preparation of products for microscopy methods

Extraction of mineral particles from Cosmetics

Version 1

1 Aim & Scope

The aim of this SOP is to describe a mineral charge extraction protocol using solvents applied to cosmetic matrix.

Although allowing the detection of nanoparticles, direct observation of finished product by EM does not readily give access to particle size distribution. To circumvent this limitation, extraction of particles from the organic matrix, prior to the determination of particle size distribution, by means of EM or other techniques, has been investigated. Three samples were delivered to the ND consortium: *i* ID 13a is the actual representative sample, containing 4% NanoTiO2, with an aluminum salt based surface treatment, as a UV filter, plus: micro-Titanium and Iron oxides for coloring purpose; *ii* ID 13b, is a simplified formula, containing 4% NanoTiO2, with an aluminum salt based surface treatment, as a UV filter (same particles as for ID 13a); iii A blank formula, without mineral particles (noted ID blank) has been provided. ID 13b and ID blank were delivered to the Consortium for the purpose of helping for the extraction of Nano-particles from ID 13a. The organic components are identical for the three samples.

2 Definitions

Rpm	round per minute
QSF	quantity sufficient for
g	gravitational factor
FFP3	Filtering Facepiece Particles 3
Dry ice	frozen CO_2
Vortex mixer	allow to mix liquid +solid with vibration
Centrifugal apparatus	allow to separate solid and liquid
Magnetic stirrer	allow to mix liquid and solid with mechanic movement
PTFE	Polytetrafluoroethylene (chemically inert)

3 Description

3.1 Materials and methods

Centrifugal apparatus: SIGMA supplier/ SIGMA centrifuge 3 K 30/ controlled temperature system (setpoint temperature to 23°C) / max 28200rpm / equipped with 12155 rotor 4x 85ml - max radius 9cm-min radius 2,1cm-angle 30°-max speed 20000 rpm- max gravitational 40248g / AUREAU VERITAS controlled every years

Vial for centrifugal: SIGMA supplier /Polycarbonate tube 85ml standard screw cap diameter 38x104mm

Vortex mixer apparatus: Heidolph supplier/ REAX2000 / 2400 x 1/min

Magnetic stirrer apparatus: 2mag magnetic^{e}motion supplier / MIX15

Rod for magnetic stirrer: PTFE coated ovoid shape in order to fit to the bottom centrifugal polycarbonate tube

Ultrasound bath apparatus: Bransonic supplier / US Bransonic 3510E-DTH, 100W 42 KHZ ± 6%

Solvents used:

- Absolute Ethanol - VWR Chemicals supplier/ AnalaR NORMAPUR –ref 20821.296

-Water for HPLC - CARLO ERBA supplier / filtered through 0.1µm membrane

Freeze dryer apparatus: Thermo Supplier / Lyolab A

Freezing mix: dry ice + acetone (normal quality)

Weighing apparatus: METTLER supplier / AT261 deltaRANGE scale / 205g to 0,1mg or 62g to 0,01mg

3.2 Sample preparation

3.2.1 Sample preparation

Particle extraction protocol:

In a centrifuge tube (60ml /polycarbonate)

- Add magnetic stirrer (ovoid shape)
- weight 5g of finished product
- Add absolute ethanol (QSF: 50g)

Cycle 1

- Vortex mixer: 30 seconds
- Magnetic stirrer: 15 min (700 rpm)
- Ultrasonic bath: 15 min
- Centrifugation; 20 000 g (14026rpm): 15min
- Remove slowly the liquid phase
- Add absolute ethanol to solid phase residue (QSF: 50g)

Cycle 2 = Cycle 1

Cycle 3 = Cycle 1

Cycle 4

- Vortex mixer: 30 seconds
- Magnetic stirrer: 15 min (700 rpm)
- Ultrasonic bath: 15 min
- Centrifugation; 20 000 g: 15min
- Remove slowly the liquid phase

- Add 30ml of water
- Magnetic stirrer: 5 min (700 rpm)

- Pour into a freeze drying flask (rinsing out with 10 ml of water)

- Freeze the dispersion with a bath full of a mix of dry ice and acetone
- Freeze drying during 12h.

3.2.2 Measurement description

The insoluble fractions have been weighted for the three products, and corresponding percentage determined in mass:

ID 13a: the insoluble fraction corresponds to 11.1% of the initial formula

ID 13b: the insoluble fraction corresponds to 7.7% of the initial formula

ID blank (blank formula): the insoluble fraction corresponds to 3.3% of the initial formula

4 HSE issues

Solvent absolute Ethanol:

Highly flammable liquid and vapour- keep away from hot surface, sparks and other ignition sources- take precautionary measures against static discharge- wear protective gloves/ protective clothing/ eyes protection/ face protection.

Extractions residue: due to containing nanoparticles

- Wear protective gloves/ protective clothing/ eyes protection/ face protection/ mask protective FFP3.

- Place weighing apparatus in a protective area like an Erlab laboratory hood / Captair flex XLS 392 with 2 filter HEPA UP17

Ultrasound apparatus: use EAR protection

Freezing mix (dry ice + acetone):

-Dry ice: due to the low temperature (-78°C) wear temperature protective gloves/ protective clothing/ eyes protection/ face protection.

-Acetone: Highly flammable liquid and vapour- keep away from hot surface, sparks and other ignition sources- take precautionary measures against static discharge- wear protective gloves/ protective clothing/ eyes protection/ face protection.

Appendix D References

R. Ruiz, A. I. Martinez, A. A. López, A. Barrañon, Study of Superparamagnetic Nanocomposites of High Density Polyethylene and Maghemite *Advanced Applications of Electrical Engineering,* ISSN 1790-5117, ISB 978-960-474-072-7 2009 219-221.

J.P. Gaviría, A. Bohé, A. Pasquevich , D.M. Pasquevich, *Hematite to magnetite reduction monitored by Mössbauer spectroscopy and X-ray diffraction, Physica B, 389, 2007, 198-201*

H. Gnägi, D. Studer, E. Bos, P. Peters, J. Pierson, Ultramicrotomy in biology and materials science: an overview, *EMC 2008 14th European Microscopy Congress 1–5 September 2008*, Aachen, Germany, pp 797-798

R. J. Young, M. V. Moore, Dual-Beam (FIB-SEM) Systems, *Introduction to Focused Ion Beams*, Chapter 12, ed. L. A. Giannuzzi, F. A. Stevie, 2005, Springer US, pp 247-268

P. A. Midgley, R. E. Dunin-Borkowski, *Electron tomography and holography in materials science*, Nature Materials 8, 271-280, 2009

